US 20250257499A1

(19) United States

(12) Patent Application Publication (10) Pub. No.: US 2025/0257499 A1

Thippanna et al. (43) Pub. Date: Aug. 14, 2025

(54) **COAXIAL LAYERED FIBER SPINNING FOR WIND TURBINE BLADE RECYCLING**

(71) Applicants: **Varunkumar Thippanna**, Tempe, AZ (US); **Arunachalam Ramanathan**, Tempe, AZ (US); **Dharneedar Ravichandran**, Tempe, AZ (US); **Kenan Song**, Athens, GA (US)

(72) Inventors: **Varunkumar Thippanna**, Tempe, AZ (US); **Arunachalam Ramanathan**, Tempe, AZ (US); **Dharneedar Ravichandran**, Tempe, AZ (US); **Kenan Song**, Athens, GA (US)

(21) Appl. No.: **19/053,118**

(22) Filed: **Feb. 13, 2025**

Related U.S. Application Data

(60) Provisional application No. 63/552,993, filed on Feb. 13, 2024.

Publication Classification

(51) **Int. Cl.**

D01F 8/18	(2006.01)
D01D 5/06	(2006.01)
D01D 5/34	(2006.01)
D01D 10/02	(2006.01)
D01F 8/08	(2006.01)
D01G 11/00	(2006.01)

(52) **U.S. Cl.**

CPC ***D01F 8/18*** (2013.01); ***D01D 5/06*** (2013.01); ***D01D 5/34*** (2013.01); ***D01D 10/02*** (2013.01); ***D01F 8/08*** (2013.01); ***D01G 11/00*** (2013.01); *D10B 2101/06* (2013.01); *D10B 2321/10* (2013.01); *D10B 2401/063* (2013.01)

(57) **ABSTRACT**

Recycling wind turbine blades includes shredding, crushing, and milling the wind turbine blades to yield a multiplicity of particles including glass fiber and sieving the particles to yield a multiplicity of pellets including glass fibers. Manufacturing a composite coaxial fiber includes providing a first, second, and third polymer composition to yield a composite coaxial fiber precursor, processing the composite coaxial fiber precursor to yield a coagulated composite coaxial fiber precursor, drawing the coagulated composite coaxial fiber precursor, and heating the drawn coagulated composite coaxial fiber precursor to yield the composite coaxial fiber. The second polymer composition can include the recycled glass fibers. The resulting composite coaxial fiber includes an inner and outer layer including polyacrylonitrile and a middle layer between the inner layer and the outer layer. The middle layer includes polyacrylonitrile and a multiplicity of the recycled glass fibers.

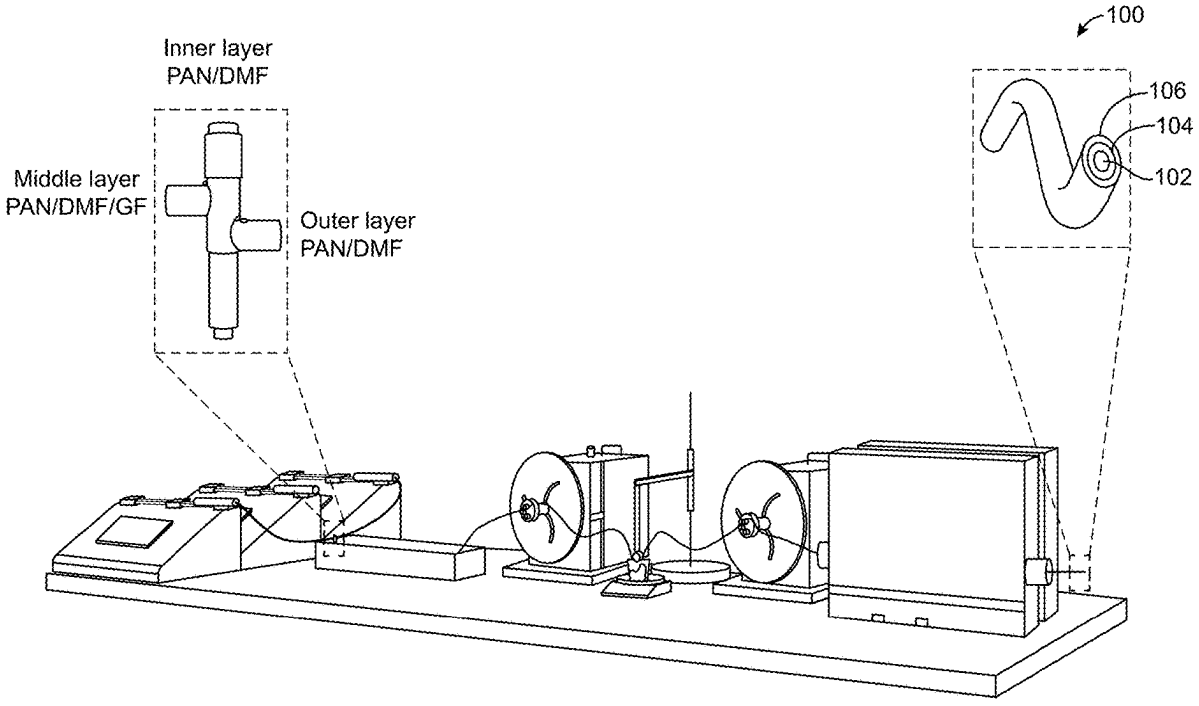

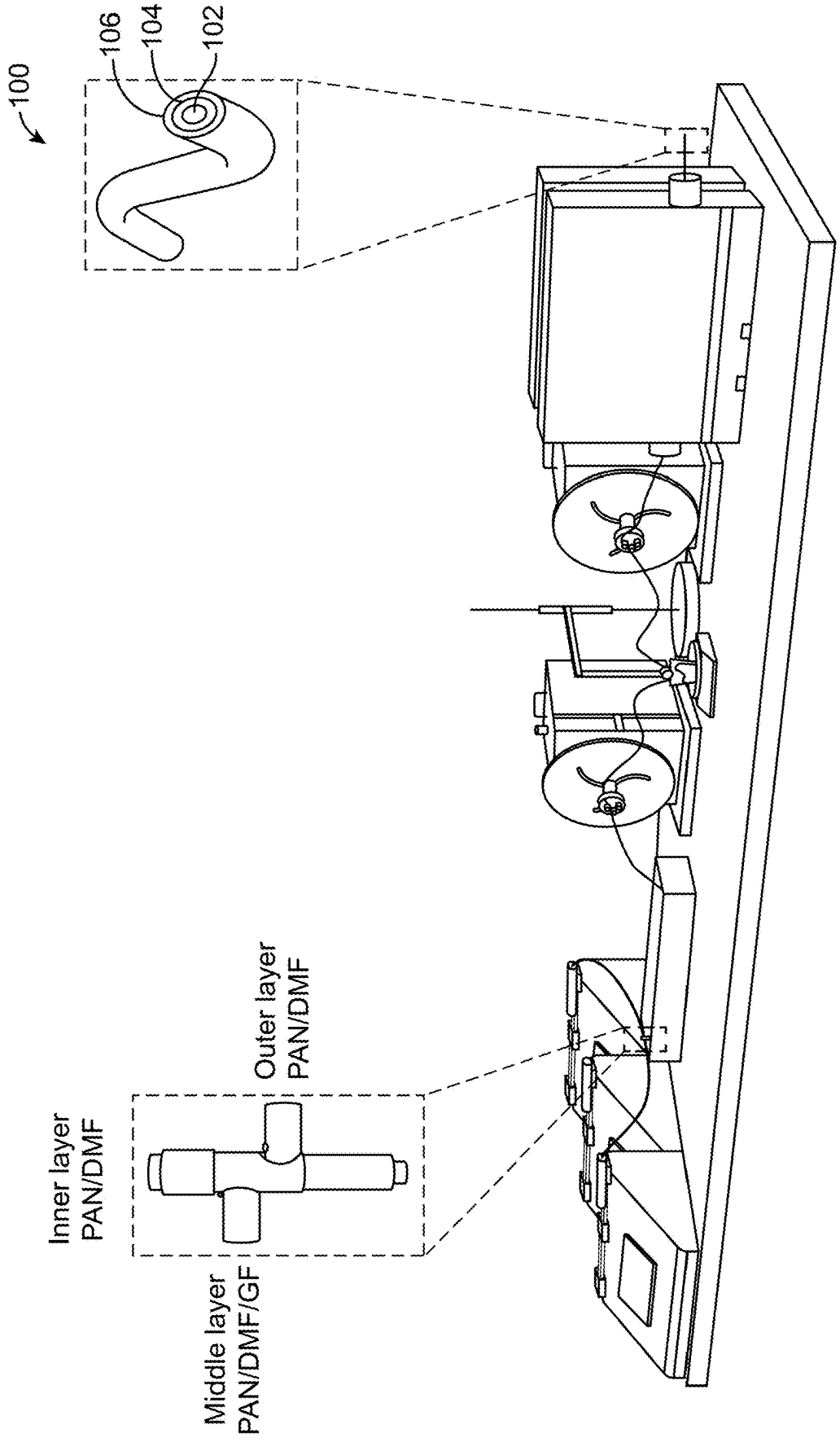
100
106
104
102
Outer layer
PAN/DMF
Inner layer
PAN/DMF
Middle layer
PAN/DMF/GF

FIG. 1A

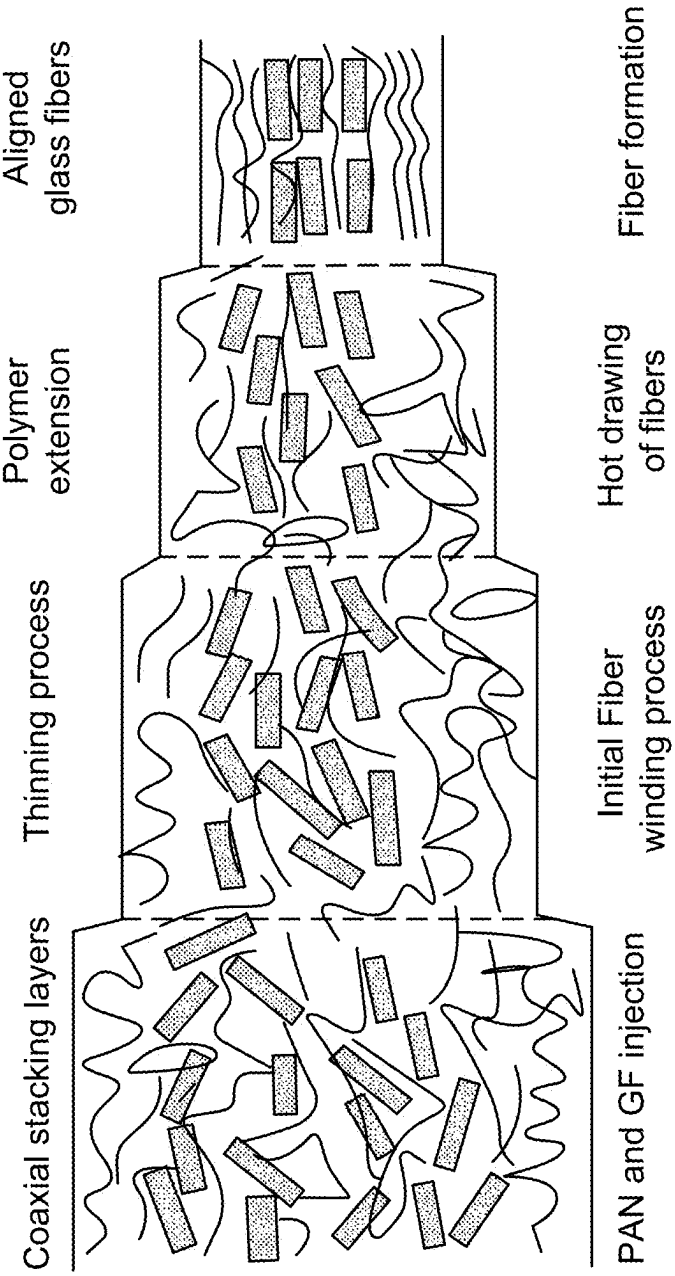
Coaxial stacking layers
Thinning process
Polymer extension
Aligned glass fibers
PAN and GF injection
Initial Fiber winding process
Hot drawing of fibers
Fiber formation

FIG. 1B

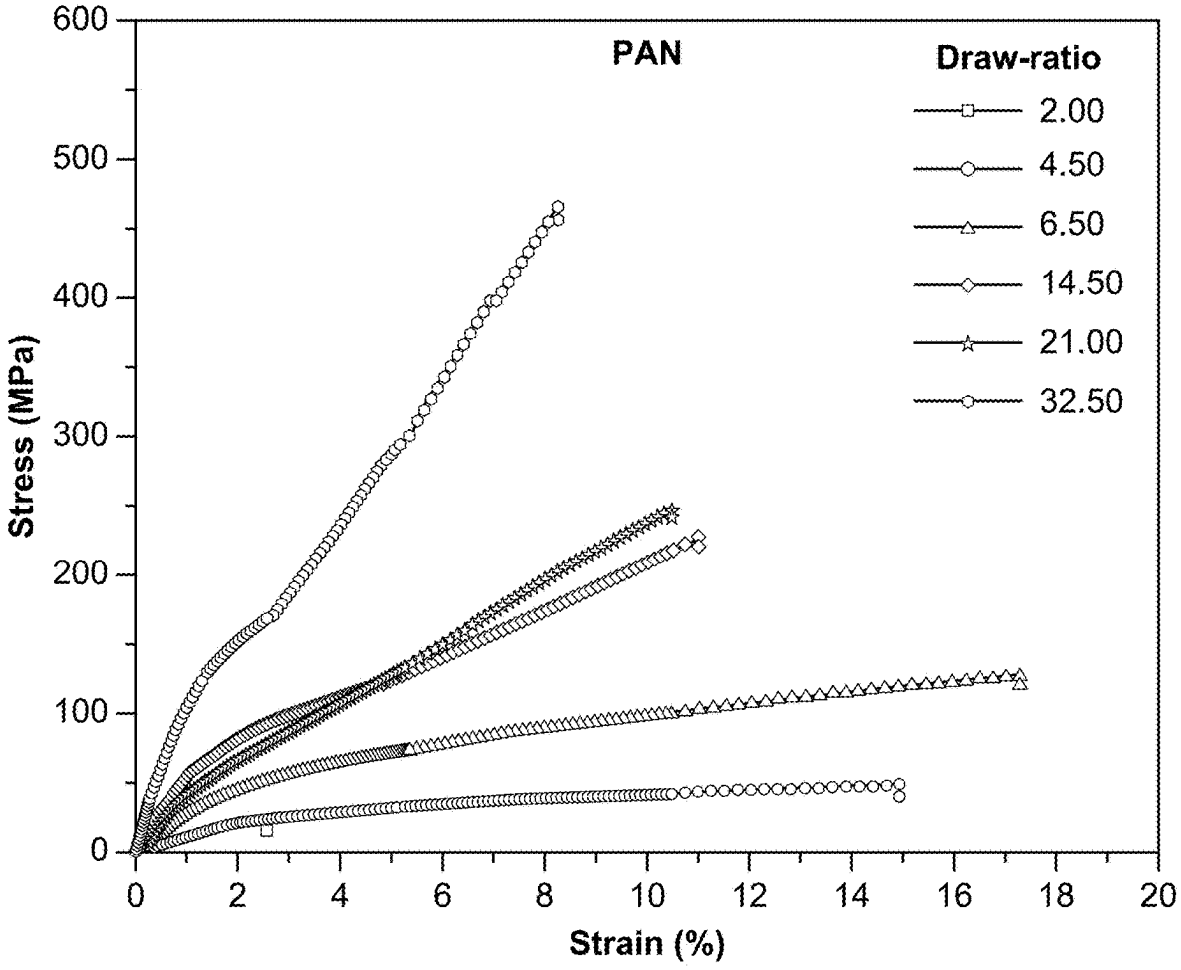
PAN
Draw-ratio
2.00
4.50
6.50
14.50
21.00
32.50
Stress (MPa)
Strain (%)
0
100
200
300
400
500
600
0
2
4
6
8
10
12
14
16
18
20

FIG. 2A

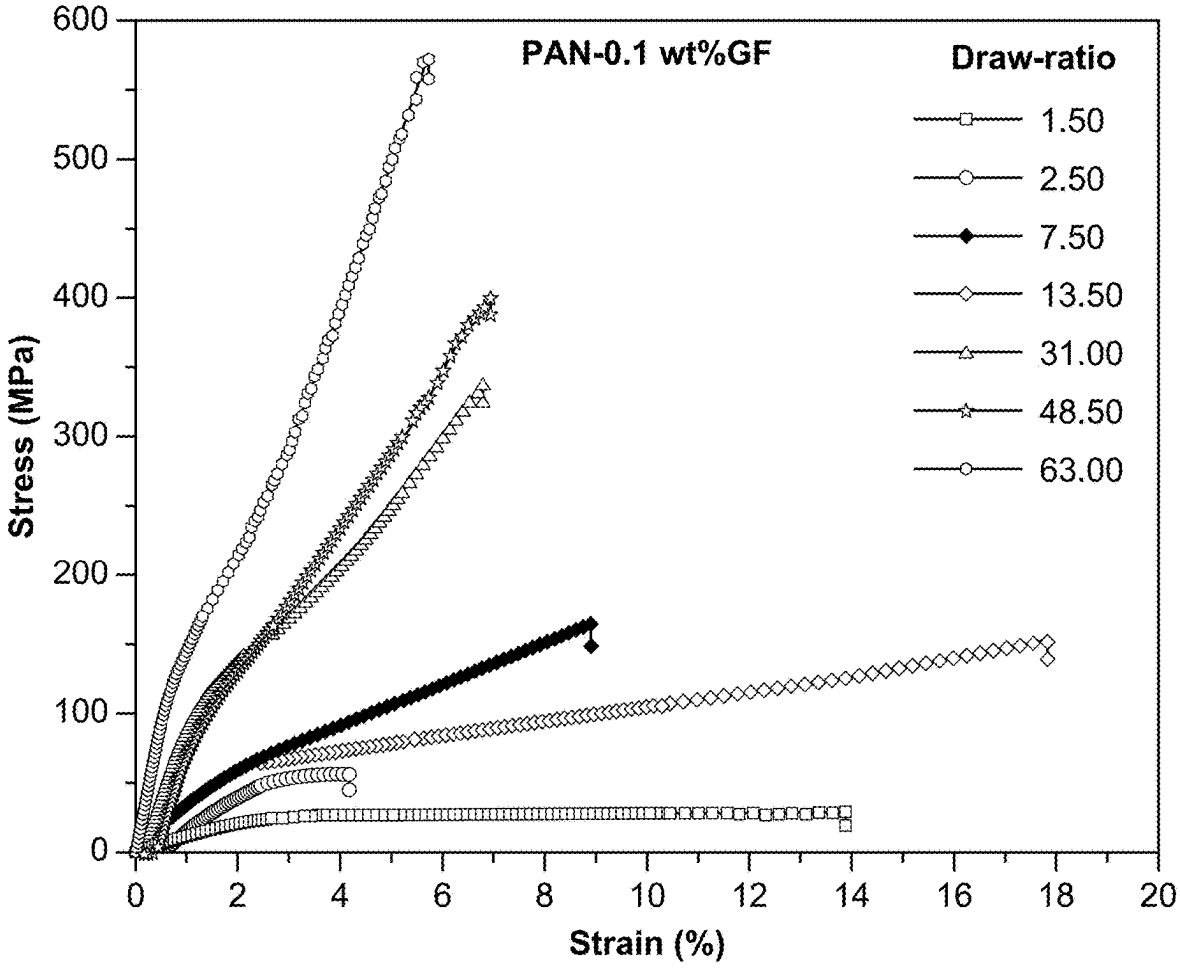
PAN-0.1 wt%GF
Draw-ratio
1.50
2.50
7.50
13.50
31.00
48.50
63.00
Stress (MPa)
Strain (%)
0
100
200
300
400
500
600
0
2
4
6
8
10
12
14
16
18
20

FIG. 2B

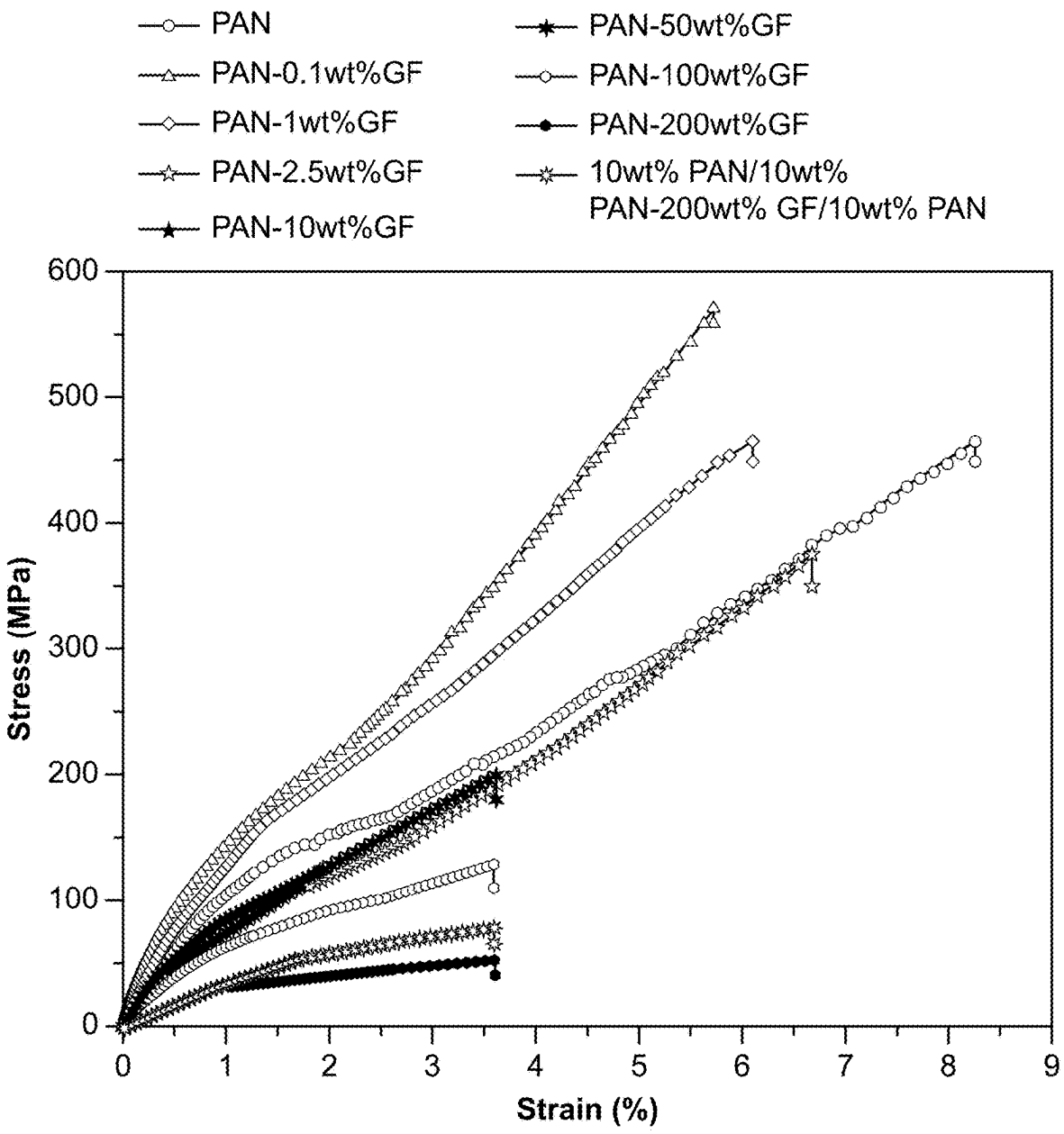
PAN
PAN-0.1wt%GF
PAN-1wt%GF
PAN-2.5wt%GF
PAN-10wt%GF
PAN-50wt%GF
PAN-100wt%GF
PAN-200wt%GF
10wt% PAN/10wt% PAN-200wt% GF/10wt% PAN
Stress (MPa)
Strain (%)
0
100
200
300
400
500
600
0
1
2
3
4
5
6
7
8
9

FIG. 2C

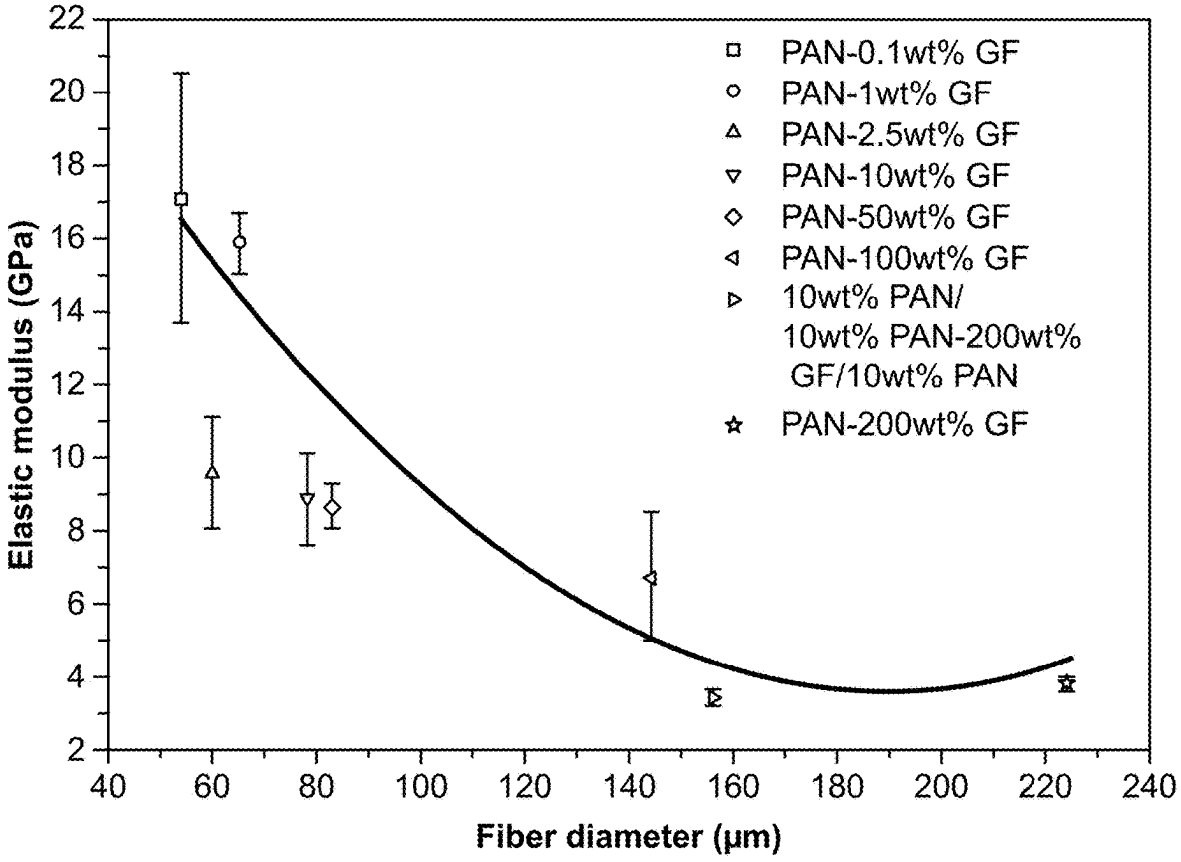
Elastic modulus (GPa)
Fiber diameter (μm)
PAN-0.1wt% GF
PAN-1wt% GF
PAN-2.5wt% GF
PAN-10wt% GF
PAN-50wt% GF
PAN-100wt% GF
10wt% PAN/
10wt% PAN-200wt%
GF/10wt% PAN
PAN-200wt% GF

FIG. 2D

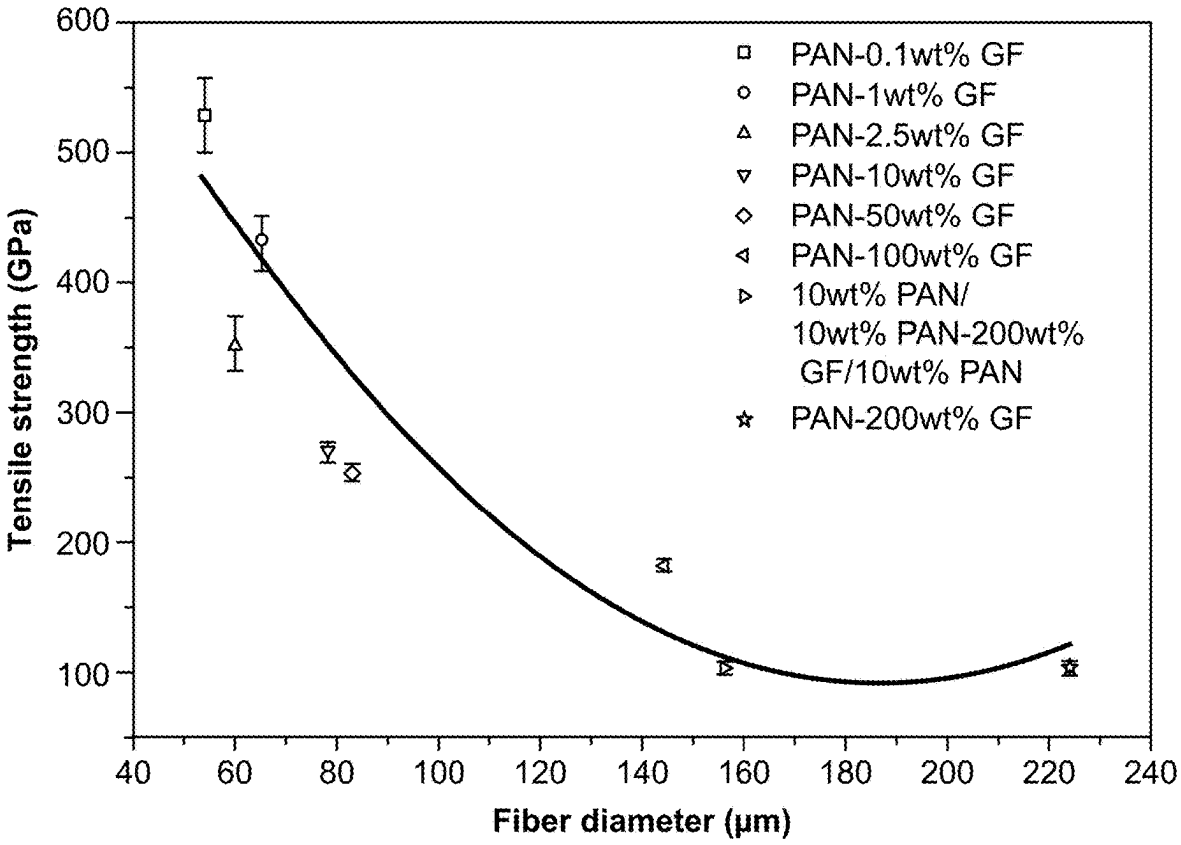
Tensile strength (GPa)
600
500
400
300
200
100
40
60
80
100
120
140
160
180
200
220
240
Fiber diameter (μm)
PAN-0.1wt% GF
PAN-1wt% GF
PAN-2.5wt% GF
PAN-10wt% GF
PAN-50wt% GF
PAN-100wt% GF
10wt% PAN/
10wt% PAN-200wt%
GF/10wt% PAN
PAN-200wt% GF

FIG. 2E

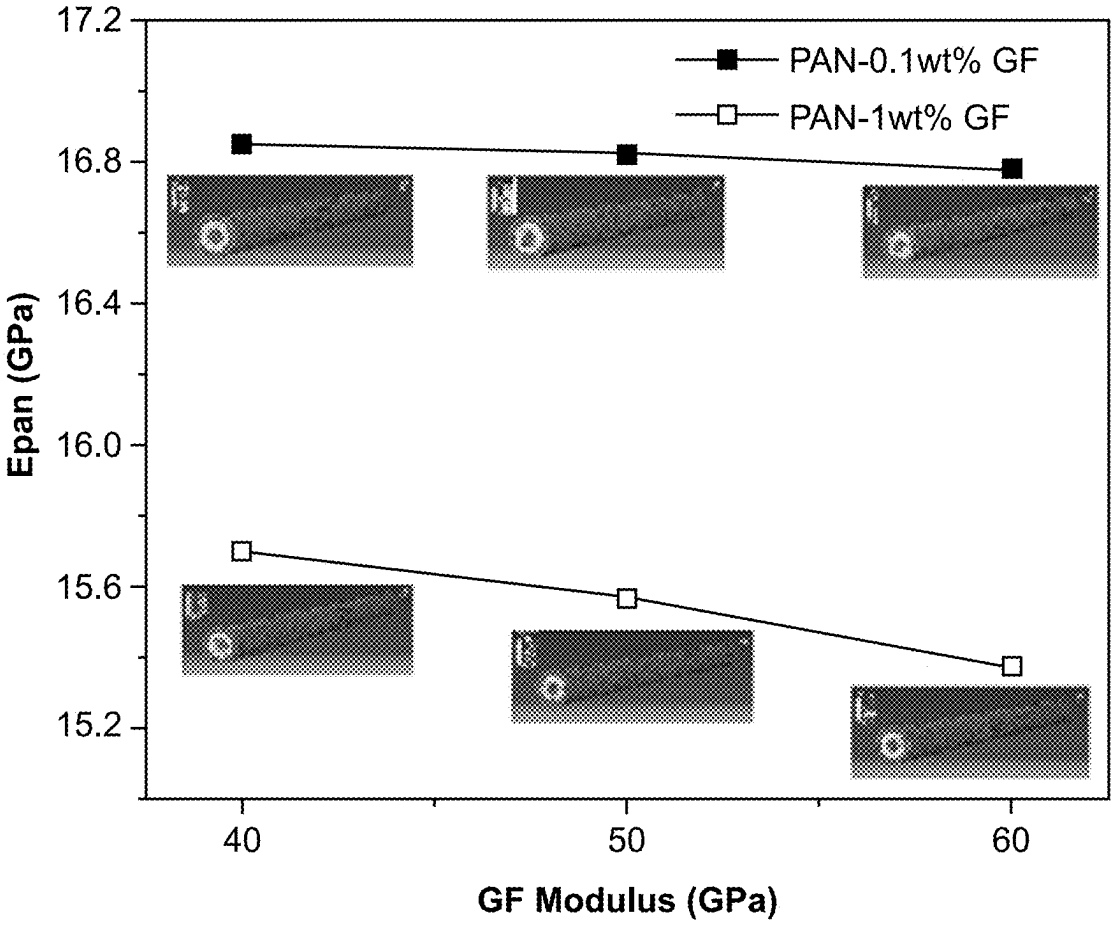
17.2
16.8
16.4
16.0
15.6
15.2
Epan (GPa)
40
50
60
GF Modulus (GPa)
PAN-0.1wt% GF
PAN-1wt% GF

FIG. 2F

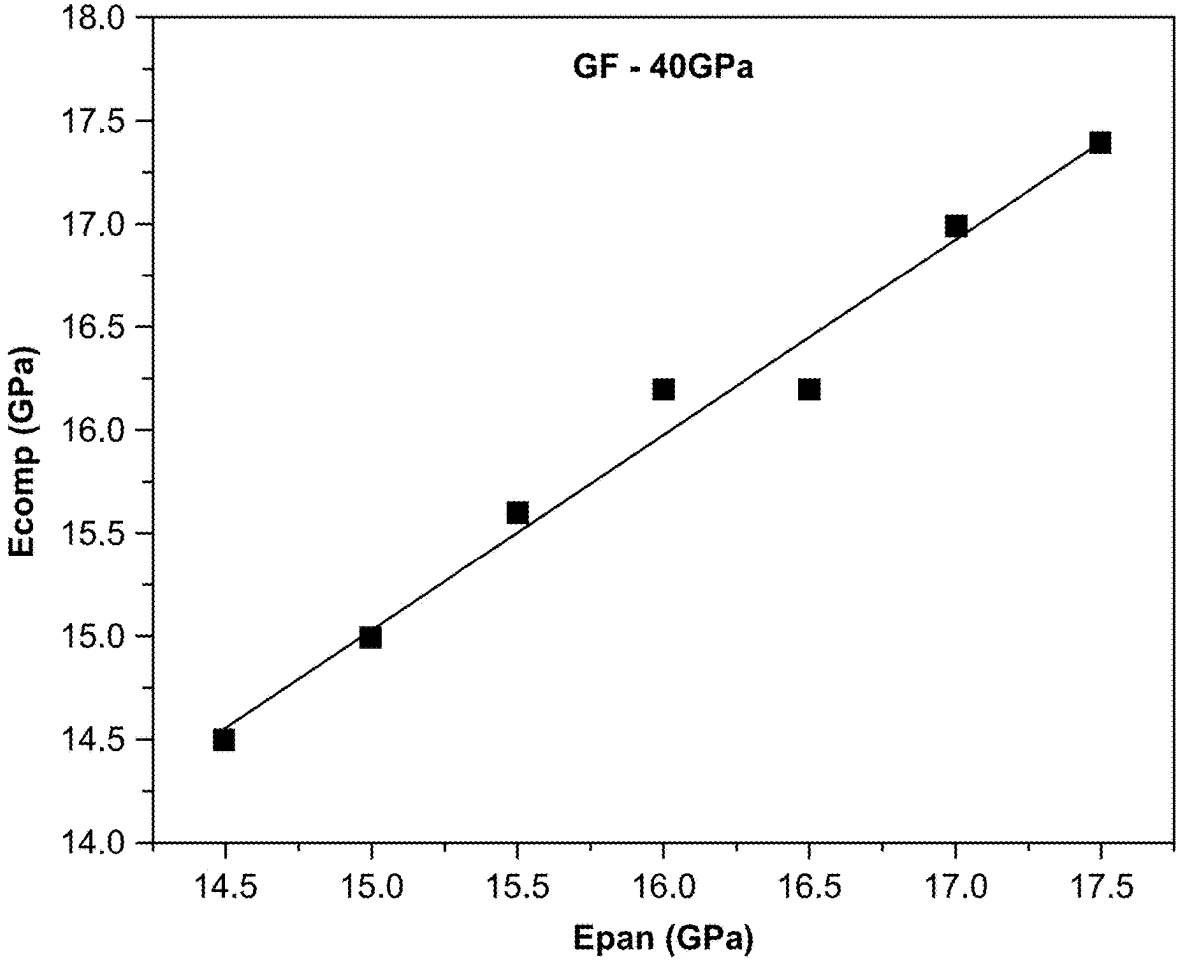
GF - 40GPa
Ecomp (GPa)
Epan (GPa)
18.0
17.5
17.0
16.5
16.0
15.5
15.0
14.5
14.0
14.5
15.0
15.5
16.0
16.5
17.0
17.5

FIG. 2G

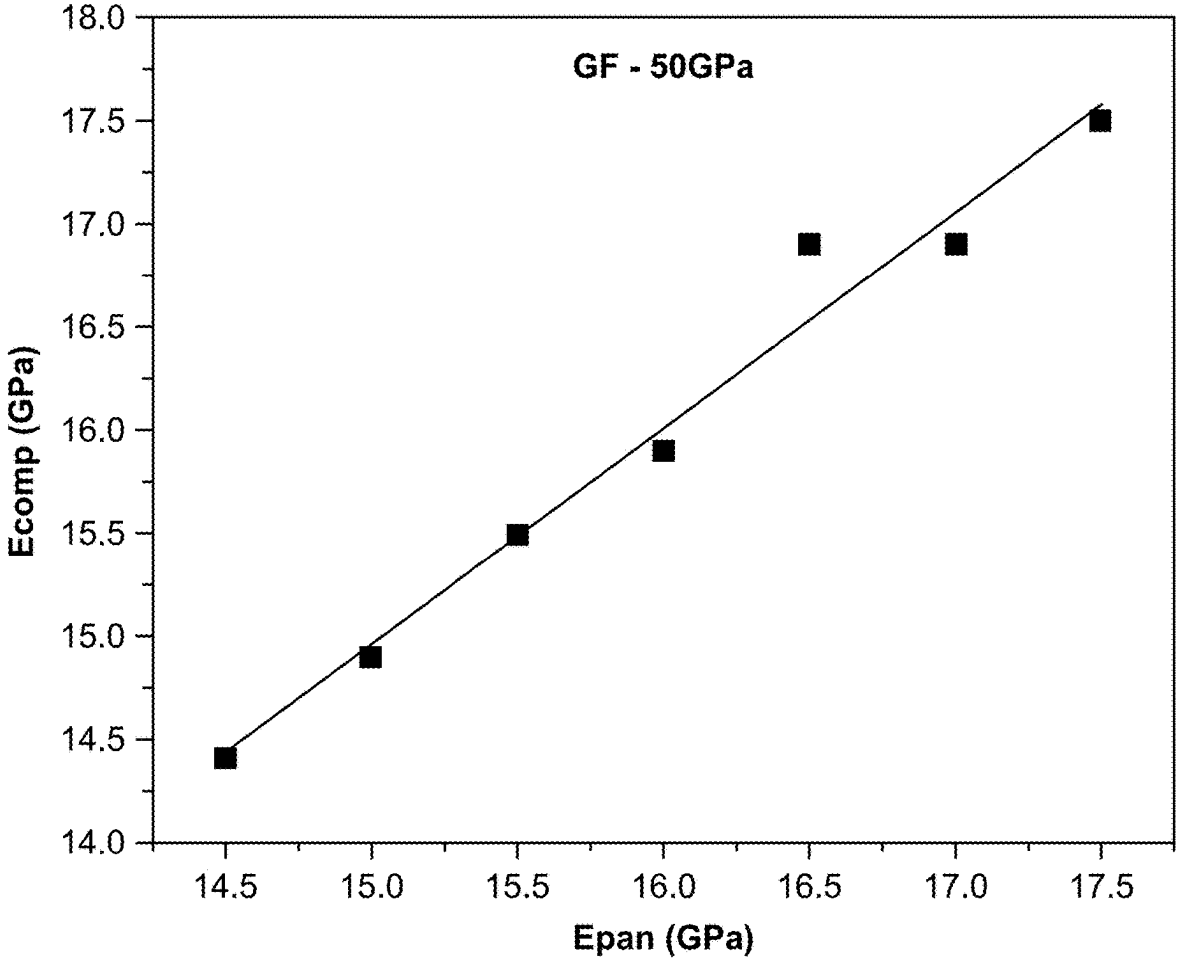
GF - 50GPa
Ecomp (GPa)
Epan (GPa)
18.0
17.5
17.0
16.5
16.0
15.5
15.0
14.5
14.0
14.5
15.0
15.5
16.0
16.5
17.0
17.5

FIG. 2H

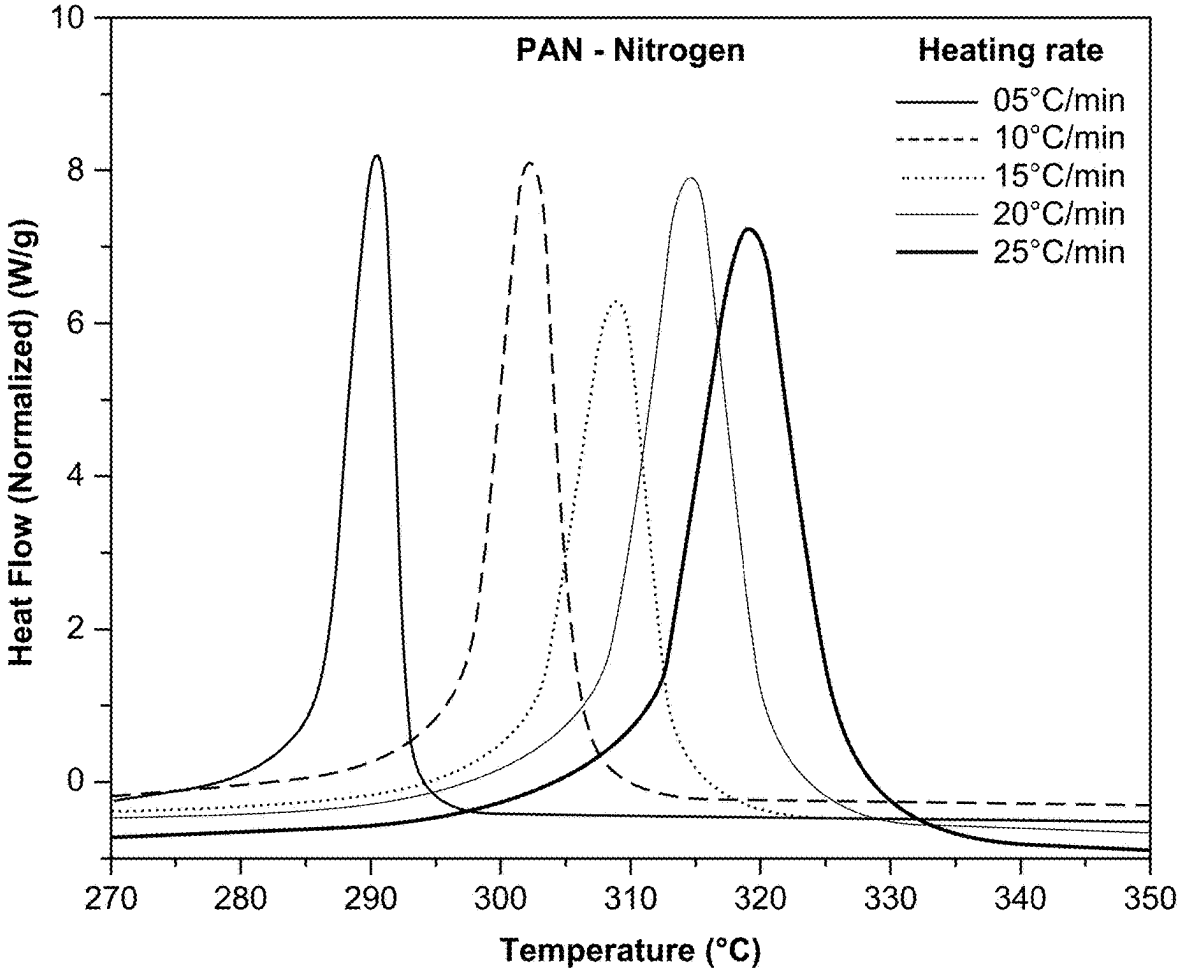
PAN - Nitrogen
Heating rate
05°C/min
10°C/min
15°C/min
20°C/min
25°C/min
Heat Flow (Normalized) (W/g)
Temperature (°C)
10
8
6
4
2
0
270
280
290
300
310
320
330
340
350

FIG. 3A

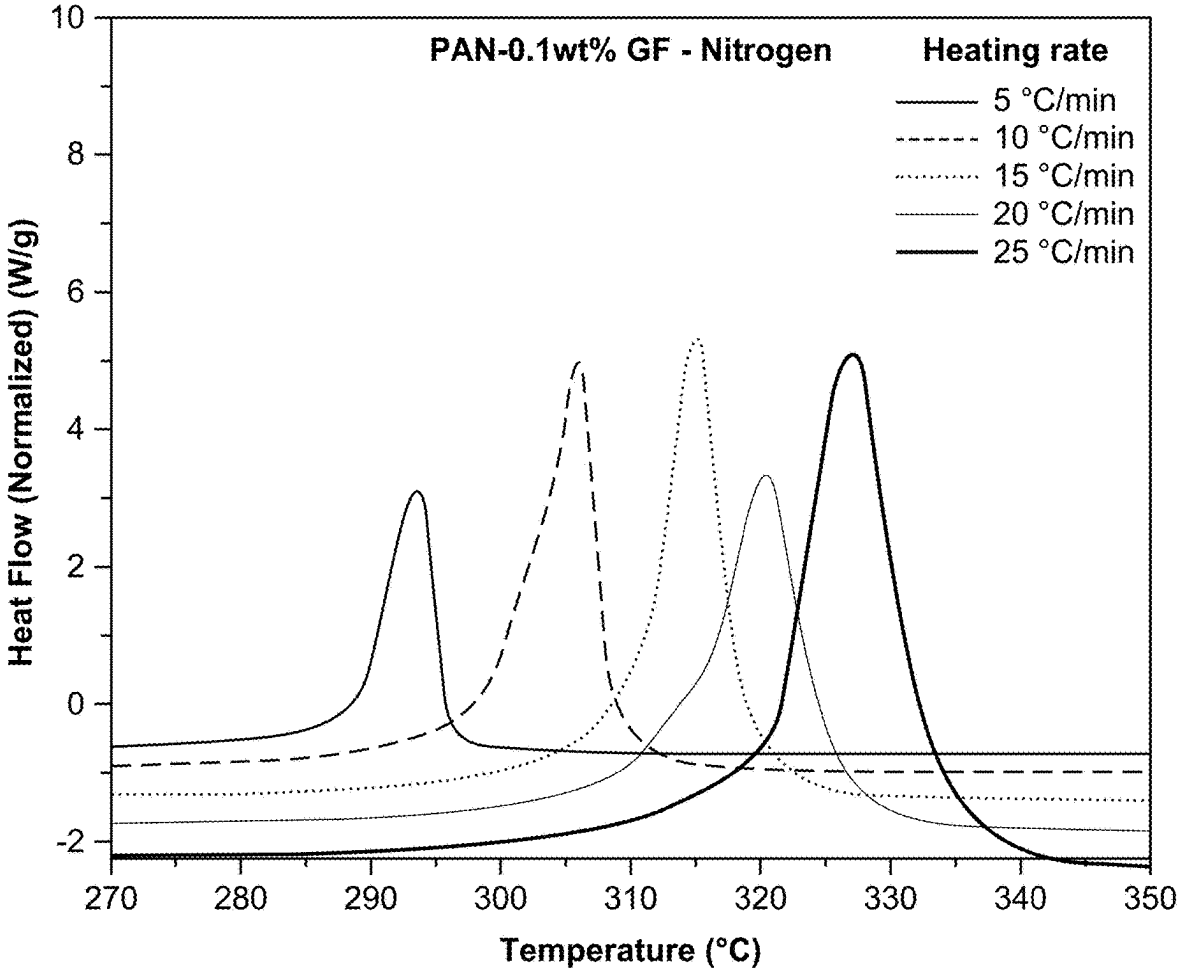
PAN-0.1wt% GF - Nitrogen
Heating rate
5 °C/min
10 °C/min
15 °C/min
20 °C/min
25 °C/min
Heat Flow (Normalized) (W/g)
Temperature (°C)
10
8
6
4
2
0
-2
270
280
290
300
310
320
330
340
350

FIG. 3B

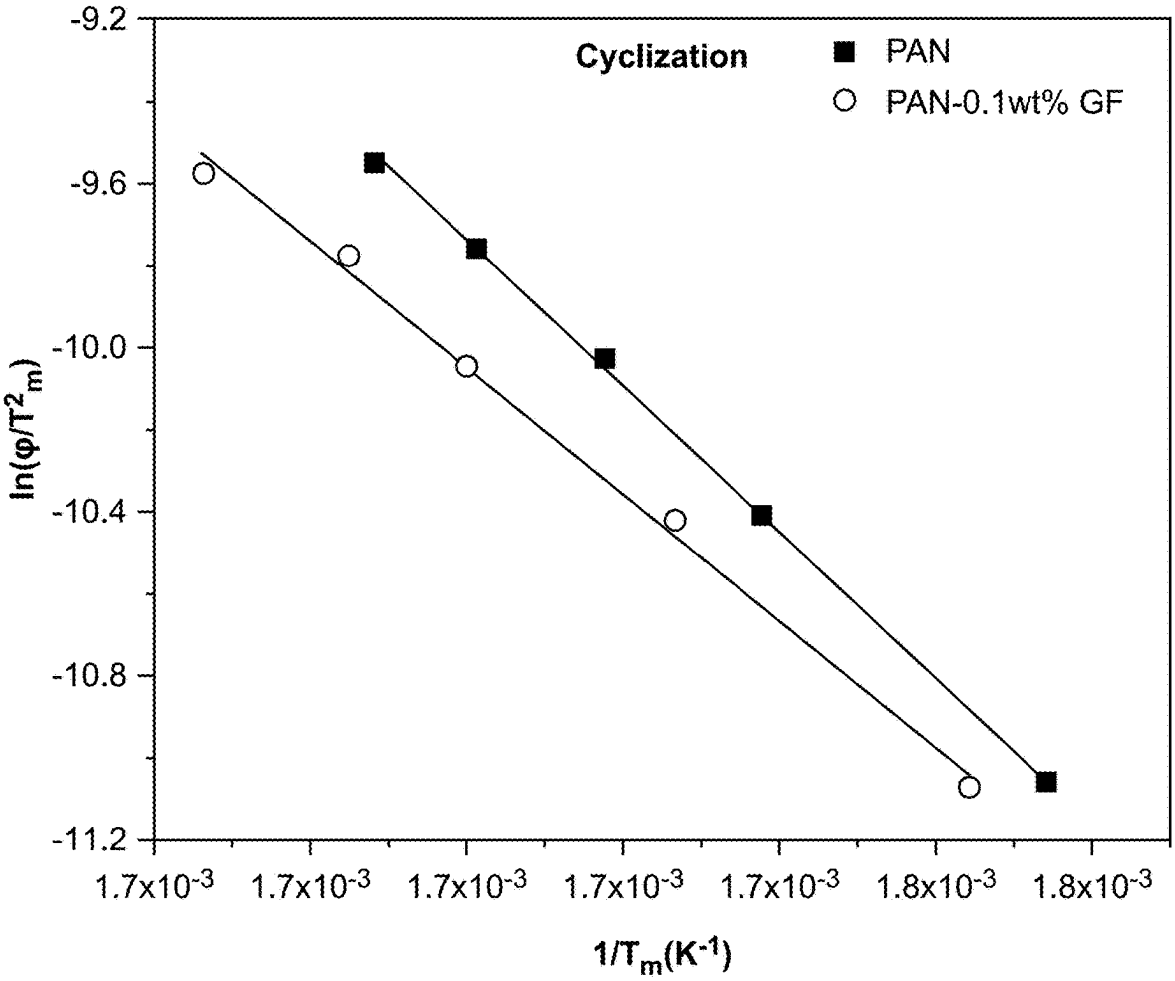
Cyclization
PAN
PAN-0.1wt% GF
-9.2
-9.6
-10.0
-10.4
-10.8
-11.2
ln(φ/T²m)
1.7x10-3
1.7x10-3
1.7x10-3
1.7x10-3
1.7x10-3
1.8x10-3
1.8x10-3
1/Tm(K-1)

FIG. 3C

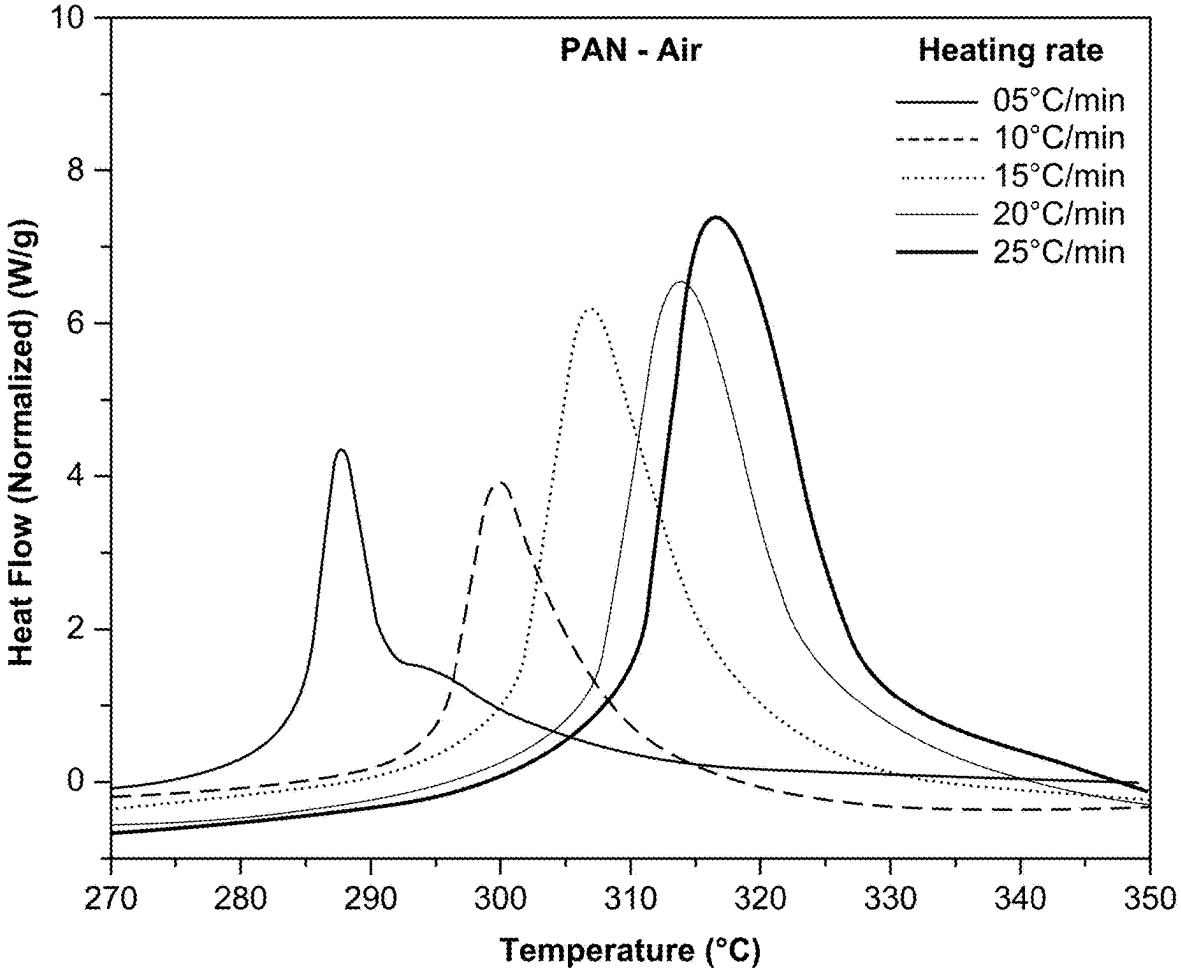
PAN - Air
Heating rate
05°C/min
10°C/min
15°C/min
20°C/min
25°C/min
Heat Flow (Normalized) (W/g)
Temperature (°C)
10
8
6
4
2
0
270
280
290
300
310
320
330
340
350

FIG. 3D

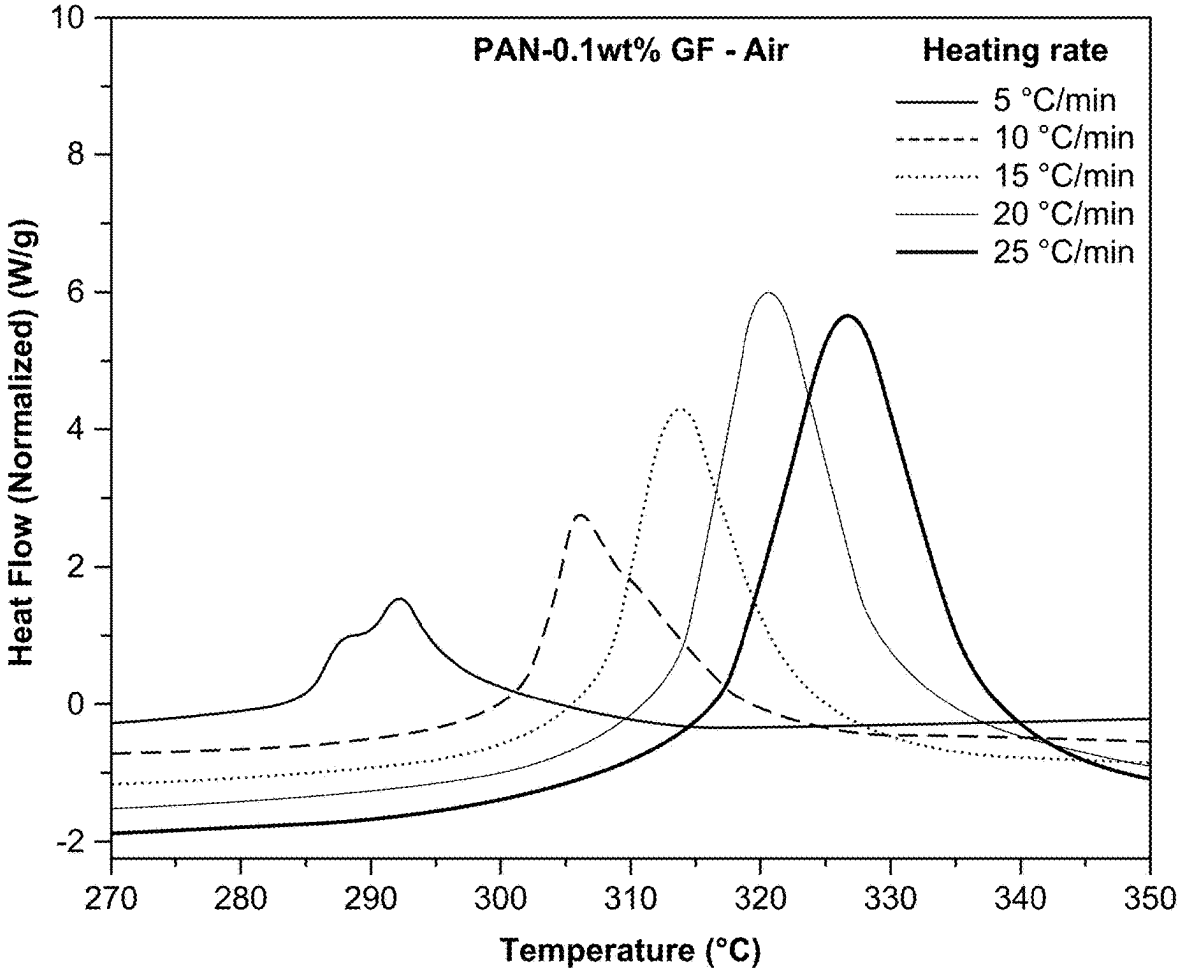
PAN-0.1wt% GF - Air
Heating rate
5 °C/min
10 °C/min
15 °C/min
20 °C/min
25 °C/min
Heat Flow (Normalized) (W/g)
Temperature (°C)
10
8
6
4
2
0
-2
270
280
290
300
310
320
330
340
350

FIG. 3E

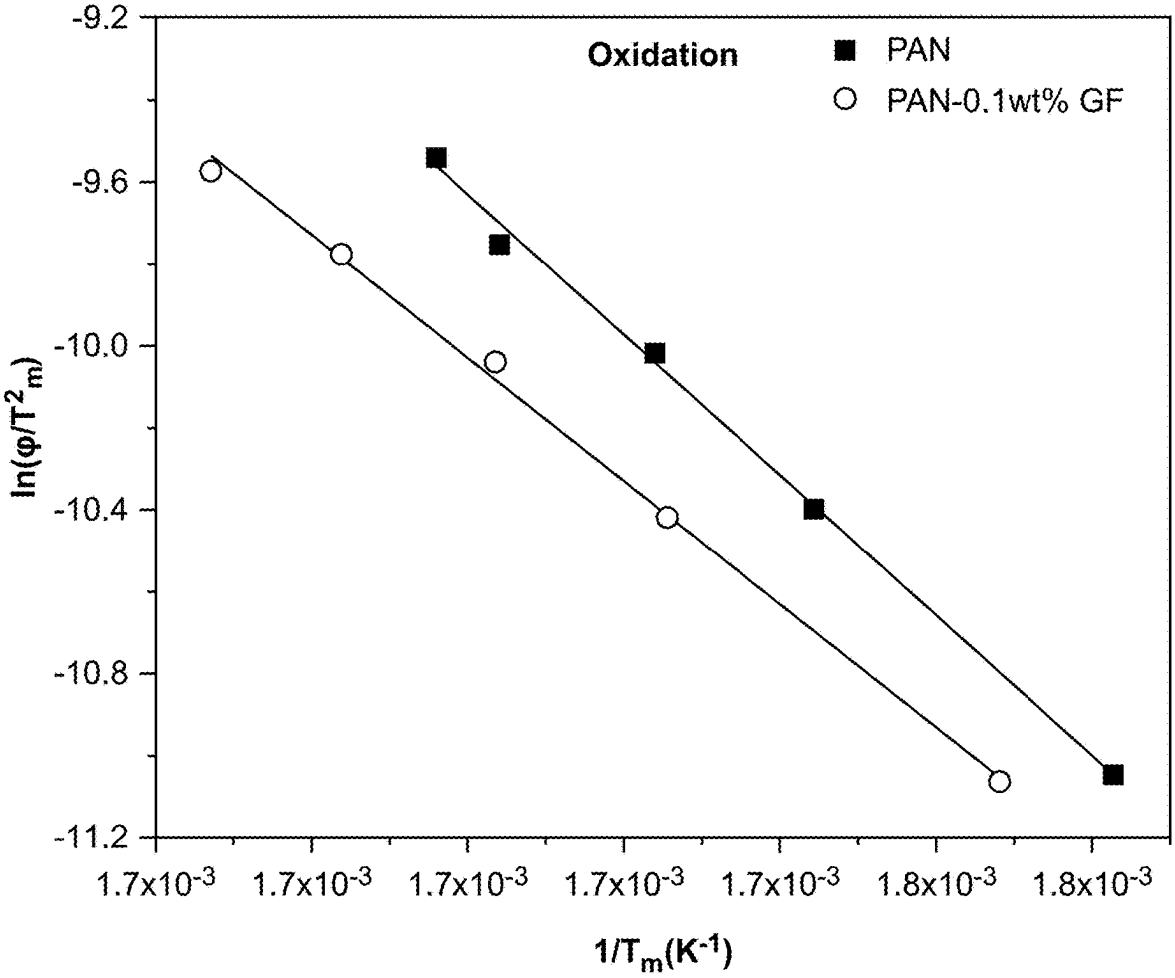
Oxidation
PAN
PAN-0.1wt% GF
-9.2
-9.6
-10.0
-10.4
-10.8
-11.2
ln(φ/T²m)
1.7x10-3
1.7x10-3
1.7x10-3
1.7x10-3
1.7x10-3
1.8x10-3
1.8x10-3
1/Tm(K-1)

FIG. 3F

COAXIAL LAYERED FIBER SPINNING FOR WIND TURBINE BLADE RECYCLING

CROSS-REFERENCE TO RELATED APPLICATION

[0001] This application claims the benefit of U.S. Patent Application No. 63/552,993 filed on Feb. 13, 2024, which is incorporated herein by reference in its entirety.

STATEMENT OF GOVERNMENT SUPPORT

[0002] This invention was made with government support under 2132183 awarded by the National Science Foundation. The government has certain rights in the invention.

TECHNICAL FIELD

[0003] This invention relates to a method of recycling composite wind turbine blades and recovering valuable glass fibers to obtain coaxial layered fibers.

BACKGROUND

[0004] The majority of wind turbine blade waste is currently disposed of in landfills. However, this is not an environmentally sustainable solution. Recycling techniques for glass fiber-reinforced plastics used in wind turbine blades currently encompass three processes: mechanical, thermal, and chemical. Mechanical recycling, which is the most widely used, involves breaking down the composite material and reducing particle size through shredding, crushing, milling, and sieving.

SUMMARY

[0005] This disclosure describes methods of recycling composite wind turbine blades and recovering glass fibers (GF). The GF are suitable for use as a feedstock for polyacrylonitrile (PAN)/GF coaxial-layered fibers. Smaller diameter fiber improves composite material performance by reducing defects and enhancing mechanical properties. A relationship is observed between fiber diameter and experimental modulus and strength, with smaller-diameter fibers demonstrating superior performance.

[0006] In a first general aspect, a composite coaxial fiber includes an inner layer including polyacrylonitrile, an outer layer including polyacrylonitrile, and a middle layer between the inner layer and the outer layer. The middle layer includes polyacrylonitrile and a multiplicity of recycled glass fibers.

[0007] Implementations of the first general aspect can include one or more of the following features. The multiplicity of glass fibers are typically present in an amount of 0.1 wt % to 200 wt % of the polyacrylonitrile in the middle layer. In some cases, a diameter of the composite coaxial fiber is in a range of about 50 μm to about 250 μm. The middle layer can have a thickness corresponding to the thickness of a single glass fiber. The glass fibers are aligned along a longitudinal axis of the composite coaxial fiber. A draw ratio of the composite coaxial fiber can be in a range of about 15 to about 65.

[0008] In a second general aspect, manufacturing a composite coaxial fiber includes providing a first polymer composition, a second polymer composition, and a third polymer composition to a spinneret to yield a composite coaxial fiber precursor. The first, second, and third polymer compositions include polyacrylonitrile, and the second polymer composition further includes recycled glass fibers. A layered precursor includes coaxial layers of the first, second, and third polymer compositions. A middle layer of the composite coaxial fiber precursor includes the second polymer composition. Manufacturing a composite coaxial fiber includes passing the composite coaxial fiber precursor through an air gap and into a coagulation bath to yield a coagulated composite coaxial fiber precursor, and drawing the coagulated composite coaxial fiber precursor through a heated liquid to align the recycled glass fibers in a middle layer of the coagulated composite coaxial fiber precursor, thereby yielding a drawn coagulated composite coaxial fiber precursor. The drawn coagulated composite coaxial fiber precursor is heated to yield the composite coaxial fiber. An inner layer, the middle layer, and an outer layer of the composite coaxial fiber includes polyacrylonitrile, and the middle layer further includes the aligned recycled glass fibers.

[0009] Implementations of the second general aspect can include one or more of the following features. The first, second, and third polymer compositions typically include about 5 wt % to about 15 wt % polyacrylonitrile in a solvent. In some cases, the solvent includes dimethylformamide. The second polymer composition can include about 0.1 wt % to about 200 wt % of the recycled glass fibers with respect to the weight of the polyacrylonitrile. A flow rate of passing the composite coaxial fiber precursor through an airgap and into a coagulation bath is typically in a range of about 1 ml/min to about 3 ml/min. In some cases, a length of the air gap is about 1 cm to about 3 cm. The coagulation bath can include methanol. In one example, the heated liquid includes a water, an oil bath, or both, with fibers being drawn separately in each in water and oil baths at their respective temperatures. The water can be heated, for example, to 80° C. to 95° C. (e.g., 85° C.), while the oil is heated to a temperature range of approximately 120° C. to 150° C. The oil bath typically includes (or consists of) silicone oil.

[0010] In some cases, a draw ratio of the coagulated composite coaxial fiber precursor is in a range of about 15 to about 65. Heating the drawn coagulated composite coaxial fiber can include heating the drawn coagulated composite coaxial fiber to a temperature in a range of about 250° C. to about 350° C. (e.g., at different heating rates for 1.5 hr and later cooled to room temperature at a rate of 1° C./min to produce stabilized fibers). A diameter of the composite coaxial fiber can be in a range of about 50 μm to about 250 μm.

[0011] In a third general aspect, recycling wind turbine blades includes shredding, crushing, and milling the wind turbine blades to yield a multiplicity of particles including glass fiber, and sieving the multiplicity of particles to yield a multiplicity of pellets including glass fiber.

[0012] The PAN/GF coaxial-layered fibers manufactured herein demonstrate superior mechanical properties and are lightweight in nature, surpassing pure PAN polymer. This advancement offers a sustainable solution for composite material development, with substantial increases in both strength and modulus. These fibers are suitable for applications such as body panels and chassis components for electric vehicles.

[0013] The details of one or more embodiments of the subject matter of this disclosure are set forth in the accompanying drawings and the description. Other features,

aspects, and advantages of the subject matter will become apparent from the description, the drawings, and the claims.

BRIEF DESCRIPTION OF DRAWINGS

[0014] FIG. **1**A is a schematic diagram depicting a manufacturing process for fabricating 3-layered composite fibers. The manufacturing process depicts material delivery via syringes and syringe pumps, a coagulation bath, a water and oil bath for temperature and anti-oxidation control via fiber winders, and a tube furnace for post-drawing treatment. The left inset of FIG. **1**A shows an exemplary spinneret. The right inset of FIG. **1**A shows a representative coaxial fiber structure with layers. FIG. **1**B is a schematic diagram of an evolution of polymer chains during fiber spinning and drawing procedures.

[0015] FIGS. **2**A-**2**H show mechanical properties of drawn fibers. FIG. **2**A shows polyacrylonitrile (PAN) fibers showing increasing mechanical properties (e.g., strength, modulus) as a function of the increasing draw ratio. FIG. **2**B shows PAN-0.1 wt % glass fibers (GF) showing increasing mechanical properties with increasing draw ratios. FIG. **2**C shows the effect of increasing GF concentrations on the mechanical properties, showing the highest increase in 0.1 wt % GF addition as compared with pure PAN after the drawing procedures. FIGS. **2**D and **2**E show the elastic modulus and tensile strength values, respectively, as a function of the fiber diameter. FIG. **2**F shows simulation results of Young's modulus of bulk PAN in the composites, with the Young's modulus higher for 0.1 wt % and 1 wt % GF addition than the 14.55 GPa in pure PAN fibers for, suggesting the influence of GF on PAN morphologies and microstructures. FIG. **2**F shows the mechanical contribution from PAN in the composite, calculated based on the tested composite properties, glass fiber and PAN percentage, and parametric studies of GF modulus (e.g., 40, 50, and 60). FIGS. **2**G and **2**H show a GF modulus of 40 GPa and 50 GPa, respectively, would generate the composite modulus.

[0016] FIGS. **3**A-**3**F show differential scanning calorimetry curves in nitrogen atmosphere with different heating rates. FIG. **3**A shows PAN and FIG. **3**B shows PAN-0.1 wt % GF. FIG. **3**C shows plots of $\ln(\varphi/T_m^2)$ versus $1/T_m$ according to the Kissinger method for PAN and PAN/GF fibers, in cyclization. FIGS. **3**D and **3**E, respectively, show differential scanning calorimetry curves in air with different heating rates for PAN and PAN-0.1 wt % GF, respectively. FIG. **3**F shows plots of $\ln(\varphi/T_m^2)$ versus $1/T_m$ according to the Kissinger method for PAN and PAN/GF fibers, in oxidation reaction kinetics.

DETAILED DESCRIPTION

[0017] This disclosure describes recycling wind turbine blades to recover glass fibers (GF) from wind turbine blades. The method includes shredding, crushing, and milling the wind turbine blades to yield a multiplicity of particles including GF, and sieving the particles to yield a multiplicity of pellets including GF. The recovered GF can be used as particle fillers in the fabrication of coaxial layered fibers. This disclosure also describes the production of polyacrylonitrile (PAN)/PAN-GF/PAN coaxial-layered fibers, achieved by a dry-jet wet-spinning technique. The process includes passage of polymer compositions through a 3-phase spinneret, followed by immersion in a methanol bath to ensure controlled solvent exchange. The obtained fibers are subsequently subjected to a drawing process in in separate water and oil baths at an elevated temperature to align the polymer and induce complete crystallization. The resulting fiber, which incorporates ≥0.1 wt % GF within the middle layer, demonstrates enhancements in mechanical properties over PAN fibers. PAN-based fibers can be combined with various fillers, including glass fibers, metals, and particles, to create composites that allow tailoring of mechanical properties.

[0018] FIG. **1**A depicts a method of manufacturing a composite coaxial fiber. The method includes providing a first polymer composition, a second polymer composition, and a third polymer composition to a spinneret to yield a composite coaxial fiber precursor, as shown in the left inset of FIG. **1**A. The method includes passing the composite coaxial fiber precursor through an air gap and into a coagulation bath to yield a coagulated composite coaxial fiber precursor, drawing the coagulated composite coaxial fiber precursor through a heated liquid to yield a drawn coagulated composite coaxial fiber precursor, and heating the drawn coagulated composite coaxial fiber precursor to yield the composite coaxial fiber **100**, as shown in the right inset of FIG. **1**A.

[0019] The first, second, and third polymer compositions used in the manufacturing of a composite coaxial fiber includes about 5 wt % to about 15 wt % polyacrylonitrile in a solvent. The solvent can include dimethylformamide. The second polymer composition further includes about 0.1 wt % to about 200 wt % of the recycled GF with respect to the weight of the polyacrylonitrile. A layered precursor includes coaxial layers of the first, second, and third polymer compositions.

[0020] In one example, a flow rate of passing the composite coaxial fiber precursor through an airgap and into a coagulation bath is in a range of about 1 ml/min to about 3 ml/min, and a length of the air gap is about 1 cm to about 3 cm. The coagulation bath can include methanol. The heated liquid includes separate oil and water baths at their respective temperatures. One example of a suitable oil is silicone oil. A temperature of the water bath is in a range of about 80° C. to about 90° C. A temperature of the oil bath is in a range of about 120° C. to about 150° C. A draw ratio of the coagulated composite coaxial fiber precursor in a range of about 15 to about 65. Heating the drawn coagulated composite coaxial fiber includes heating the drawn coagulated composite coaxial fiber to a temperature in a range of about 250° C. to about 350° C. to yield the composite coaxial fiber (e.g., at different heating rates for 1 to 2 hours and later cooled to room temperature at a rate of about 1° C./min to yield stabilized fibers).

[0021] The right inset of FIG. **1**A depicts a composite coaxial fiber **100**. The composite coaxial fiber **100** includes an inner layer **102**, a middle layer **104**, and an outer layer **106**. The inner layer **102** and outer layer **106** includes polyacrylonitrile. The middle layer **104** includes polyacrylonitrile and a multiplicity of recycled glass fibers. The multiplicity of glass fibers are present in an amount of 0.1 wt % to 200 wt % of the polyacrylonitrile in the middle layer **104**. The middle layer **104** has a thickness corresponding to the thickness of a single glass fiber. The multiplicity of glass fibers are aligned along a longitudinal axis of the composite coaxial fiber. A draw ratio of the composite coaxial fiber **100**

is in a range of about 15 to about 65. A diameter of the composite coaxial fiber is typically in a range of about 50 μm to about 250 μm.

EXAMPLES

Materials and Methods

[0022] Polyacrylonitrile (PAN) copolymer (e.g., 99.5% acrylonitrile/0.5% methacrylate) with a molecular weight of 230,000 g/mol and a mean particle size of 50 μm was obtained from Goodfellow Cambridge Limited, Huntingdon England. Wind turbine blades containing glass fiber-reinforced plastics were obtained from TPI Composites, Inc., (Iowa, US). These glass fiber-reinforced plastics were mechanically recycled through shredding, crushing, milling, and sieving (via the mesh **40**) to obtain pellet samples with an average particle size of 38 μm. N,N-dimethylformamide (DMF) (ACS reagent, ≥99.8%) was used as a solvent to dissolve PAN and the media to disperse glass fiber powder. Methanol (ACS reagent, ≥99.8%) was used as the coagulant. Solvents were obtained from Sigma-Aldrich, US. All materials were purchased and used as received without further modifications.

Characterizations

[0023] Single fiber uniaxial tests were conducted using a tensile tester (Discovery HR-2 hybrid rheometer, TA Instruments Inc., USA). A gauge length of 20 cm was used with a constant linear strain rate of 50 μm/s for fibers drawn at different stages. 5-7 samples of each fiber type were tested to obtain the mechanical parameters, including Young's modulus, tensile strength, tensile strain, and toughness. Differential Scanning calorimetry (DSC) (DSC 250, TA Instruments Inc., USA) was conducted on 2 mg fiber samples for each fiber type, and the temperature increased from room temperature (~25° C.) to 370° C. with a different heating rate of 5-25° C./min in a nitrogen atmosphere to understand the cyclization behaviors, followed by reruns in the air for oxidation and crosslinking studies. The filler (e.g., glass fibers (GF)) dispersion in the polymer (e.g., PAN) and the fiber morphological features of different PAN/GF concentrations were observed using scanning electron microscopy (e.g., scanning electron microscopy/Focused Ion Beam, Auriga (Zeiss)) at an operating voltage of 5 kV. All the fibers were mounted on a 90° cross-sectional stub with a fractured surface facing up and were coated with a thin gold layer (15-20 nm) before scanning electron microscopy imaging.

Example 1. Preparation of 1-Phase and 3-Phase Fibers

[0024] Preparation of 1-phase feedstock: A PAN solution was made by dissolving 12 g of PAN in 100 ml DMF solvent. The resulting mixture was mechanically stirred at a temperature of 130° C. for 1 hour until a transparent solution was obtained. To remove any trapped air, the solution was de-aerated in a vacuum oven (Lindberg Blue M lab oven, Thermo Scientific US) for 30 minutes, ensuring a bubble-free solution. Subsequently, the solution was transferred into a metal syringe that was connected to a pump for the fiber-spinning process. The solution was injected into the spinneret at a controlled rate of 2 ml/min, facilitating the extrusion and formation of PAN comparison fibers.

[0025] Preparation of 3-layered PAN/PAN-GF/PAN feedstock: The 3-layered fibers include a coaxial layer. The spinning setup includes a coaxial spinneret responsible for producing interior, middle, and exterior layers. This coaxial spinneret was manufactured via a metal three-dimensional printer, Concept Laser 2 using Inconel. Both interior and exterior layers were filled with 12 wt % PAN solutions, as shown in Table 1. As shown in Table 1, different GF filler concentrations (e.g., 0.1 wt %-200 wt % GF with respect to PAN) were dissolved in the middle layer in 12 wt % PAN in the form of suspensions, which were obtained through tip sonication for 30 minutes at an amplitude of 60% (Q500, Fisher Scientific, US), with the same PAN/DMF solution preparation procedure as mentioned in the 1-phase PAN fibers. All the solutions were transferred into the metal syringe(s) attached to the pumps and injected at rates of 2 ml/min for the interior, middle, and exterior layers to form the 3-phase composite fibers.

TABLE 1

Summary of fiber type[a], compositions, processability and testability, and drawing parameters

		Compositions (wt %)						Drawing results	
		Interior and exterior layer	Middle layer	Middle layer	Processability and testability			Total	
Type[a]	Fiber	PAN comp. on in DMF (wt %)	PAN wt % in DMF	(GF wt % w.r.t PAN)	Spin[b]	Heat treatment	Mechan. Testab.[c]	Draw ratio	Thickness (μm)
1	PAN	12	12	0	Yes	Fiber drawing at 85° C. in water and at 125° C., 135° C. and 145° C. in silicone oil before stabilization in tube furnace	Yes	32.50	83
3	PAN-0.1 wt % GF			0.1	Yes		Yes	63.00	54
	PAN-1.0 wt % GF			1.0	Yes		Yes	41.00	65
	PAN-2.5 wt % GF			2.5	Yes		Yes	43.50	60
	PAN-10 wt % GF			10	Yes		Yes	31.50	78
	PAN-50 wt % GF			50	Yes		Yes	17.00	83
	PAN-100 wt % GF			100	Yes		Yes	28.00	144

TABLE 1-continued

Summary of fiber type[a], compositions, processability and testability, and drawing parameters

	Compositions (wt %)							
	Interior and exterior layer	Middle layer	Middle layer	Processability and testability			Drawing results Total	
Type[a] Fiber	PAN comp. on in DMF (wt %)	PAN wt % in DMF	(GF wt % w.r.t PAN)	Spin[b]	Heat treatment	Mechan. Testab.[c]	Draw ratio	Thickness (μm)
PAN-200 wt % GF			200	Yes		Yes	28.00	224
10 wt % PAN/10 wt % PAN-200 wt % GF/10 wt % PAN	10	10	200	Yes		Yes	20.00	156

[a]type refers to phase (1 or 3);
[b]spinnability;
[c]mechanical testability

[0026] Fiber spinning: During the fiber spinning process, the solution was injected in an air gap of 1.5-2.0 cm before entering the coagulation bath. The use of an air gap in dry-jet wet-spinning allowed fibers to undergo extension, reducing defect density and enabling molecular alignment. After immersing in the coagulation bath, two diffusion processes occurred simultaneously, with (i) a polymer-rich phase condensed into the fiber and (ii) a solvent-rich phase (e.g., DMF) exchanging with the non-solvent (e.g., methanol) to form the more solid-like gel fiber. As-spun fibers were soaked in methanol for 30 minutes. In the coagulation process, the coagulation rate was sufficiently high to minimize the gradient between coagulated layers from the surface to the fiber core. Consistent coagulated structures prevented deformation towards the core, resulting in a circular shape. However, if the rates differed between layers, an irregular cross-sectional shape was likely to be formed due at least in part to diffusion mismatching and solid polymer gradient. The chain alignment and dimensions of as-spun fibers were also influenced by the injection/flow rates. To reduce fiber diameter and thus the defect density, higher flow rates through the coagulation bath with lower injection rates for the spinning dope were effective. However, a larger draw ratio (e.g., fiber drawing during coagulation) in the coagulant flow cannot guarantee more polymer chain alignment due at least in part to stretching and recoiling processes. High flow rates can lead to drastic stretching and severe molecular recoil, hindering alignment; thus, the injection rates were optimized to be 2 ml/min and the winder collection rates were 33 m/min.

[0027] Fiber drawing: During the hot drawing stages, fibers were drawn separately in water and silicone oil baths at their respective temperatures to their maximum draw ratios before breakage. During this process, the high shear force caused these macromolecules to align parallel to the fiber axis. Initially, fibers were drawn through a water bath (multiple water streams) at a temperature of 85° C. controlled by the hot plate to promote the polymer chain alignment and to remove the DMF solvent, and the fibers were soaked in methanol for an additional time of 24 hrs. to further coagulate the fiber. The wet PAN fiber was dried at a temperature of 50° C. under a vacuum in the oven. The moisture in the fibers was removed and the voids collapsed. The fibers were drawn in an oil bath with varying temperatures of 125° C., 135° C. and 145° C., consecutively, for a maximized molecular extension and to add a protective layer on the fibers to avoid the defects. The highest draw ratio fibers were collected on fiber winders at 145° C. To promote the orientation of GF, 3-phase fibers were drawn at these different temperatures so that the layered fiber structure encountered higher and higher temperatures, overcoming the barriers of GF rotation momentum, and the GF had more preferentially aligned morphologies along the fiber axis. PAN fibers were stretched at high temperatures to increase the degree of the molecular orientation and to eliminate internal stress, resulting in a dense structure and optimized mechanical properties.

[0028] Fiber annealing: During the post-processing of spun fibers, residual stresses from the hot drawing stage leading to microstructural imperfections and unstable/metastable conformational chain states can be eliminated to enhance the overall fiber quality and performance. As shown in Table 1, all the spinnable fibers were heat treated in an oxidative atmosphere in the tube furnace with a temperature of 250° C.-350° C. at different heating rates for 1.5 hrs. The spinnable fibers were cooled to room temperature at rate of 1° C./min to produce stabilized fibers, as shown in the right inset of FIG. **1**A.

[0029] As shown in FIG. **1**A, the spinning technique described herein, primarily used for the 12 wt % PAN and the 12 wt % PAN/GF composite fibers, was based on dry-jet wet-spinning. A coaxial spinneret was used to create a 3-layered fiber. The process started with the extrusion of spinning dope through a spinneret, with flow rates precisely controlled by syringe pumps. The emerging fibers passed through a methanol coagulation bath at room temperature (approximately 25° C.) before being collected on winders. The fibers decreased in diameter after specific hot drawing stages. This high shear force aligned macromolecules in a more parallel manner along the fiber axis. Subsequently, the fibers underwent drawing in an oil bath at varying temperatures of 125° C., 135° C., and 145° C., successively, to maximize molecular extension without oxidation and degradation, thus achieving the highest draw ratio. The fibers were then collected on fiber winders. Post-drawing procedures were carefully controlled with programmable heating

rates and temperatures via a tube furnace. The mechanical, thermal, and morphological properties of these PAN and 3-phase composite fibers were assessed. Throughout the drawing and post-treatment procedures, the exterior PAN layer was expected to form more extended polymer chains than the inner PAN layer, generating shear stress on the middle layer including GF, as shown in FIG. **1**B. Consequently, this shear stress applied during the fiber thinning process compelled better GF alignment along the fiber axis than simply mixed compositions without layered microstructure, resulting in higher mechanical reinforcement.

[0030] Table 1 lists the fiber processability, testability, and drawing parameters. All samples were spinnable, with stable quality and minimized defect density after optimizing the fabrication parameters (e.g., injection rates, air gap, flow rates in coagulant, and collection rates). The addition of GF and the effect on the fiber stretchability and dimensions were compared with the pure PAN. The draw ratio increased with proper GF additions (e.g., 0.1 wt %, 1.0 wt %, and 2.5 wt %) as compared to the pure PAN. The direct contact of the outer layer of the fiber with the hot medium led to more macromolecular stretching than the inner layer due at least in part to the heat transfer efficiency, with the GF facilitating the extension of polymer chains due at least in part to the lubrication effects in the middle layer. As a result, the stacked particles underwent stepwise exfoliation and aligned in the axial direction. The efficiency of exfoliation and alignment in the 3-phase fibers relied on the initial thickness of the channel and could be controlled by adjusting the spinneret outlet dimension and air gap distance. However, higher GF inclusions in the fiber middle layer (e.g., >2.5 wt %, as shown in Table 1) resulted in decreased drawability compared to pure PAN fibers. For example, the presence of 200 wt % GF in 12 wt % and 10 wt % PAN fibers showed a decreased total draw ratio of 28 and 20, with the final fiber diameter of 224 μm and 156 μm, respectively, both much larger than the pure PAN fibers (e.g., draw ratio of 32.5 and diameter of 83 μm).

[0031] Fiber drawability serves as a metric not only indicating processability (as presented in Table 1) but also reflecting the extent of polymer chain alignment and subsequent mechanical property developments, as illustrated in FIGS. **2**A-**2**H. The stress-strain curves, available in FIGS. **2**A-**2**C, and the corresponding mechanical property data listed in Table 2, provide valuable insights. FIG. **2**A demonstrates that PAN fibers displayed an increase in Young's modulus and ultimate tensile strength values as the draw ratio increased. In the initial phases of the drawing process, the fibers can display porosity and voids. These characteristics can lead to the formation of defects and fractures even when subjected to relatively low levels of stress. Consequently, this can lead to a decrease in the mechanical performance and strength of the fibers (low elongation break at the first few drawing stages). As the drawing process advances, with the fibers experiencing a higher draw ratio, their strength typically shows an increase. At a final stage draw ratio of 32.5 for 12 wt % PAN, the modulus reached 14.55±1.82 GPa, with a tensile strength of 460.00±15.00 MPa. These enhancements were substantial, with the modulus being 16.16 times higher and the tensile strength 23.47 times higher compared to fibers with a draw ratio of 2.00. As compared, in FIG. **2**B, the 3-phase layered fiber exhibited a similar trend of increasing modulus with the highest value reaching 17.12±3.42 GPa and tensile strength of 572.25±31.00 MPa as the draw ratio increased. It is worth mentioning that further improvements in mechanical properties can be achieved by increasing the draw ratios but reducing the windability (e.g., larger draw ratios for random fiber segments and shorter fiber collections). All fibers produced allowed for continuous collection on winders, surpassing 120 m lengths.

TABLE 2

Summary of fiber drawing and mechanical properties of fibers

	Mechanical properties of pre-stabilized fibers		
Fiber type	Young's Modulus (GPa)	Tensile Strength (MPa)	Elongation at break (%)
PAN	14.55 ± 1.82	460.00 ± 15.00	7.40 ± 1.57
PAN-0.1 wt % GF	17.12 ± 3.42	572.25 ± 31.00	5.72 ± 0.06
PAN-1.0 wt % GF	15.87 ± 0.82	465.20 ± 24.00	6.09 ± 0.72
PAN-2.5 wt % GF	9.58 ± 1.52	380.50 ± 23.00	6.73 ± 1.18
PAN-10 wt % GF	8.87 ± 1.25	289.75 ± 8.50	5.41 ± 0.46
PAN-50 wt % GF	8.67 ± 0.61	272.50 ± 7.50	4.97 ± 1.37
PAN-100 wt % GF	6.72 ± 1.75	194.30 ± 5.40	6.08 ± 0.20
PAN-200 wt % GF	3.82 ± 0.25	108.56 ± 5.45	10.86 ± 1.18
10 wt % PAN/10 wt % PAN-200 wt % GF/10 wt % PAN	3.42 ± 0.18	108.10 ± 4.50	7.76 ± 0.26

[0032] The addition of GF waste had an impact on fiber drawability, as indicated in Table 1. The addition of GF subsequently influenced the mechanical properties of the resulting composites, as shown in FIG. **2**C and Table 2. As depicted in FIG. **2**C, even with a minimal GF concentration of 0.1 wt %, the composite fibers exhibited an improvement. They displayed a modulus of 17.12±3.42 GPa and a tensile strength of 572.25±31.00 MPa compared to pure PAN fibers, which had a modulus of 14.55±1.82 GPa and a tensile strength of 460.00±15.00 MPa. However, a further increase in GF weight percentage, from 0.1 wt % to 200 wt % within the middle layer of the fiber, resulted in a decrease in both Young's modulus (e.g., with an average modulus decreasing from 17.12 GPa to 3.82 GPa) and ultimate tensile strength (e.g., with an average strength dropping from 572.25 MPa to 108.56 MPa) of the composite fibers. This suggests the potential agglomeration of GF waste and its hindrance to high molecular chain extension.

[0033] The mechanical properties are affected by the loading of glass fibers, as it involves a delicate balance between GF reinforcement and the defect density induced by GF agglomeration, as shown in Table 2. A higher GF content can lead to enhanced mechanical properties, assuming the GF is well-dispersed and interacts efficiently with the matrix. However, in the middle layer with high GF content, achieving uniform distribution can be challenging. This non-uniformity can result in friction-based sliding and crack initiation between glass fibers, ultimately reducing the mechanical integrity of the composite fiber. This challenge becomes more pronounced at extreme filler loadings, such as 200 wt % GF. The irregular dispersion and distribution of fillers play a critical role in determining the composite fiber's performance. As shown in Table 2, lower strength observed in the composite samples can be attributed to several factors. One of these factors is the presence of residual resin debris and GF segments with ineffective lengths in critical areas, increasing the likelihood of micro-

crack formation. Moreover, the uneven distribution of resin particles from the recycled turbine blades on the GF surface, particularly at GF ends, can contribute to a decrease in the ultimate strength of the composite samples. Additionally, composite samples with higher GF/PAN content typically exhibit a greater number of pores, which can compromise the overall structural integrity and reduce material strength. This is evident when comparing the 12 wt % PAN-based sample (e.g., PAN-200 wt % GF) with the 10 wt % PAN-based samples (e.g., 10 wt % PAN/10 wt % PAN-200 wt % GF/10 wt % PAN) with a more detailed fiber structure.

[0034] Reducing the direct interaction between GF and increasing the contact area between GF and the polymer matrix can be achieved by decreasing the fiber diameter, as evident in the 0.1 wt % GF samples with a diameter of 54 μm, as shown in Table 1. In some cases, this fiber size reduction results in the middle layer having a single GF thickness. During the fiber drawing process, GF bundles undergo extension and reorganization, aligning preferentially along the composite fiber axis, as shown in FIG. **1**B. Referring to FIGS. **2**D-**2**E, a correlation between smaller diameter and higher mechanical properties was observed. This observation aligns with the principles of classic fracture mechanics, with the GF concentration influencing the fiber size. According to Griffith's theory, smaller diameter fibers, as initially demonstrated in glass fibers, tend to approach theoretical predictions for tenacity and strength as defects decrease. Decreasing the diameter effectively reduces defect density, nonlinearly dependent of the fiber loadings, allowing fiber properties to approach their theoretical limits.

[0035] Recycled materials can be employed as fillers or reinforcements in industries where the incorporation level of the reinforcement or filler is limited to under 10 wt % due at least in part to the poorer quality of recycled solids than virgin materials. These lower-quality dispersions often contain agglomerations or entanglements that not only initiate cracks but also hinder polymer crystallization, impeding effective alignment. Working with low-reinforcement particle loadings, such as glass fibers, can be advantageous. Low filler additions can promote interfacial crystal growth and facilitate unique crystal structures, enabling better polymer/particle interactions and precise control over the properties of the polymer composite. Table 2 demonstrates that incorporating 0.1 wt % GF in the fiber middle layer results in improvements in the fiber's overall mechanical properties. Compared to pure PAN fibers, the composite fiber exhibits a 24.4% increase in tensile strength and a 17.66% increase in tensile modulus. However, these enhancements cannot be explained by well-known composite mechanics like the rule of mixture.

$$E_c = E_f * V_f + E_m * V_m \quad \text{(Equation 1)}$$

Here, E represents the modulus, c is the composite, f is the filler, m is the matrix, and V is the volume fraction. In this case, a 0.1 wt % GF translates to only 0.017 vol % within the entire PAN matrix, and considering the ideal GF modulus of 40-60 GPa, its contribution is negligibly low, amounting to less than 0.01 GPa. Consequently, the influences of the low-concentration GF on the PAN microstructure and performance warrant further investigation. It is worth noting that the standard deviations for lower wt % GF fibers were high, and the mechanical data were more scattered than those fibers without defects. High standard deviation in their strength indicated that the presence of defects, such as porosity and voids within the gauge length, can affect the mechanical properties of the fibers. To better understand the relationship between property defects and mechanical properties, statistical analysis techniques, such as Weibull analysis, were employed, which showed a trend with the conclusion here.

Example 2. Simulation of Elastic Regime Behavior

[0036] To investigate the impact of GF on the PAN modulus, a Finite Element Method and the ABAQUS software was used to visualize the elastic regime behavior, as shown in FIG. **2**F. This analysis was initiated by modeling the layered fiber structure in both PAN-0.1 wt % GF and PAN-1 wt % GF samples. In the model, one end was fully constrained, while the other end was subjected to a small strain. Parametric studies were conducted within ABAQUS, varying the PAN modulus values within a reasonable range, and the glass fiber modulus was programmed over a range of 40, 50, and 60 GPa. In this simulation, the GF was assumed to be fully aligned with the fiber axis, and interfacial interactions remained perfect without any debonding during mechanical deformation. Consequently, the applied mechanical strain led to the generation of stress, allowing the calculation of the modulus for the composite layers within the elastic regime. Table 2 shows fitting the composite modulus to the experimental measurements to determine the intrinsic modulus of PAN, as shown in FIGS. **2**G-**2**H for 40 GPa. As shown in Table 3, PAN's contribution to the mechanical properties in the composites exceeds that in pure PAN, suggesting that the presence of glass fibers influences PAN morphologies and microstructures. This influence can be attributed to lubrication during fiber spinning and drawing, indicating a need to understand their microstructures and thermal behavior.

TABLE 3

Comparing the Young's modulus of PAN in the composites to the pure PAN fibers per the simulated values

PAN modulus in control fibers (GPa) from experiments	PAN modulus in PAN-0.1 wt % GF (GPa) derived from simulations	PAN modulus in PAN-1 wt % GF (GPa) derived from simulations	Middle layer GF modulus (GPa)
14.55	16.85	15.70	40
	16.82	15.57	50
	16.78	15.37	60

[0037] The effect of glass fiber volume in PAN/GF composite properties is demonstrated through stress distribution. Establishing a quantitative relationship between these variables can lead to effective composite design. This relationship is further supported by comparing scanning electron microscopy images of actual samples and simulated model representative volume elements. The presence of GF clusters introduces microstructural variation, leading to variable stress distribution and elastic strain across the composite representative volume element. Additionally, an increase in fiber concentration results in the observation of tangled and misoriented fibers, causing a decrease in the elastic modulus. The influence of fiber volume content appears in both

experimental and computational scenarios. An important observation is the inverse relationship between GF volume and the composite Young's modulus. This relationship displays a linear trend, indicating a decrease in elastic modulus with increasing fiber volume. Furthermore, in regions with concentrated agglomerates, stress transmission to individual fibers can be less efficient, potentially causing stress concentrations and an overall reduction in composite stiffness.

Example 3. Kinetic Analysis of Fibers

[0038] The thermal stabilization process induces both chemical and physical changes in PAN-based fibers, as shown in Table 4. Differential Scanning calorimetry analysis was carried out to record the heat flow during thermal transitions in the polymer. Differential scanning calorimetry provides data such as peak temperatures and associated enthalpy changes. To further understand the polymer behavior, the Kissinger method was utilized, which calculates the activation energy based on the peak temperatures obtained from the differential scanning calorimetry results. Activation energy measures the energy required for specific thermal processes. The activation energy values were obtained by the Kissinger equation.

$$\frac{-E_a}{R} = \frac{d\left[\ln\left(\frac{\varphi}{T_m^2}\right)\right]}{d\left(\frac{1}{T_m}\right)} \quad \text{(Equation 2)}$$

where E_a is the activation energy (kJ/mol), φ is the heating rate (° C./min), R is the molar gas constant, and T_m is the peak temperature (K). E_a was taken as the slope of the plots.

TABLE 4

Differential Scanning Calorimetry data for PAN and PAN-0.1 wt % GF fibers

	In air		In nitrogen	
Heating rate (° C./min)/peak temperature (T_m)	PAN (° C.)	PAN-0.1 wt % GF (° C.)	PAN (° C.)	PAN-0.1 wt % GF (° C.)
5	287.76	292.41	290.47	293.63
10	300.06	306.33	302.28	305.96
15	306.91	313.80	308.94	315.05
20	313.66	320.70	314.67	320.32
25	316.43	326.62	319.13	326.96

[0039] When subjecting the fibers to increasing temperatures (up to 350° C.) with a corresponding rise in heating rate under a nitrogen atmosphere, highly crystalline fibers can display a sharp exothermic peak at a specific temperature. This peak can be attributed to the cyclization reaction, as shown in FIG. **3**A for PAN and FIG. **3**B for PAN-0.1 wt % GF. However, in an air atmosphere, the peak broadens due at least in part to the simultaneous occurrence of complex chemical reactions. At a heating rate of 5° C./min, a second peak appears, reflecting the intricate interplay of crosslinking and oxidation reactions as shown in FIG. **3**D for PAN and FIG. **3**E for PAN-0.1 wt % GF. The kinetics and activation energies of these processes were further investigated by subjecting the highest draw fibers to different heating rates (ranging from 5 to 25° C./min). Increasing the heating rate led to a shift in the peak exotherm to higher temperatures in both nitrogen and air atmospheres. This shift can be attributed to the reduced time available for the fibers to complete their reactions, resulting from increased thermal effects and thermal inertia. The addition of GF can influence the thermal behavior and elevate the peak to higher temperatures, as shown in Table 4. Different fiber types were also exposed to a progressively increasing temperature, reaching up to 350° C. in both air and nitrogen environments, and recorded the peak temperatures. A shift in the peak positions towards higher temperatures was observed, particularly in the nitrogen atmosphere.

[0040] As shown in Table 5, the PAN-0.1 wt % GF composite fiber displays a higher rate constant for the cyclization reaction when compared to pure PAN fiber. This observation can underscore the impact of additional components, such as the GF reinforcing materials, on the cyclization behavior within the composite. The activation energies are observed to decrease in the PAN-0.1 wt % GF composite fibers in comparison to pure PAN fibers, both for cyclization and oxidation, as shown in FIGS. **3**C and **3**F, respectively. Several factors can contribute to this phenomenon. In some cases, the interactions that occur between the polymer matrix and the reinforcing GF materials can affect the chemical processes within the composite, leading to alterations in the activation energies of these reactions. Moreover, changes in the thermal and mechanical properties of the composite due at least in part to the presence of GF can contribute to these observed alterations. Additionally, the interface between the polymer matrix and the GF materials can be promoting enhanced chemical reactivity, which can be another factor influencing the activation energies. Furthermore, the increase in the cyclization rate constant within the composite fiber can suggest that there is an improvement in the efficiency of the cyclization process or a higher degree of cyclization. This improvement can contribute to the formation of a more stable and ordered polymer structure, which is a factor for enhancing the overall performance and properties of the composite material.

TABLE 5

Activation energies (kJ/mol) were determined from the Kissinger method for PAN and PAN-0.1 wt % GF

Chemical reaction	PAN (kJ/mol)	PAN-0.1 wt % GF (kJ/mol)
Oxidation	157.02	120.70
Cyclization	144.20	124.70

Example 4. Analysis of Fiber Morphologies Via Scanning Electron Microscopy

[0041] The fractured surfaces of both pure PAN and the composites exhibit differences in surface morphologies, particularly in terms of the dispersion patterns of the GF fibers. The degree of alignment, as shown in scanning electron microscopy images, offers a qualitative insight into the orientation of the fibers. This orientation is a factor influencing the overall mechanical behavior and anisotropic properties of the composite. Highly drawn fibers display smaller diameters than their as-spun counterparts, regardless of fiber composition. This aligns with the data provided in

Table 1. Both PAN-0.1 wt % GF and PAN-200 wt % GF composites feature a 3-layered fiber structure, with the middle layer containing varying amounts of GF. PAN-0.1 wt % GF exhibits an even distribution of GFs in the middle layer, while PAN-200 wt % GF displays heavily agglomerated GF groups. All the GF particles are observed protruding through the cross-section, which contributes to the mechanical reinforcement along the fiber direction. In cases where the GF are homogeneously dispersed and preferentially aligned along the fiber axis, the reinforcement efficiency is higher. This can result in improvements in tensile strength, modulus, and various other mechanical properties, as shown in Table 2. Highly loaded GFs were expected to provide additional strength and stiffness, further enhancing these properties. However, excessive agglomeration, especially with increasing GF loading, creates stress concentration points. This renders the fibers more prone to failure under mechanical load. Moreover, the agglomerates hinder effective dispersion and interfacial bonding between the particles and the polymer matrix, thereby limiting the desired enhancements in material properties. The broken fiber ends protruding from the fracture surface can indicate that the fibers were longitudinally aligned in the direction of the applied force. Due at least in part to the interference of the GF with the PAN matrix, the fibers ruptured and were subsequently pulled out. This analysis of the scanning electron microscopy images can suggest the intricate relationship between fiber alignment, composite composition, and resulting mechanical properties, offering an understanding of the material's behavior under mechanical stress.

[0042] Although this disclosure contains many specific embodiment details, these should not be construed as limitations on the scope of the subject matter or on the scope of what may be claimed, but rather as descriptions of features that may be specific to particular embodiments. Certain features that are described in this disclosure in the context of separate embodiments can also be implemented, in combination, in a single embodiment. Conversely, various features that are described in the context of a single embodiment can also be implemented in multiple embodiments, separately, or in any suitable sub-combination. Moreover, although previously described features may be described as acting in certain combinations and even initially claimed as such, one or more features from a claimed combination can, in some cases, be excised from the combination, and the claimed combination may be directed to a sub-combination or variation of a sub-combination.

[0043] Particular embodiments of the subject matter have been described. Other embodiments, alterations, and permutations of the described embodiments are within the scope of the following claims as will be apparent to those skilled in the art. While operations are depicted in the drawings or claims in a particular order, this should not be understood as requiring that such operations be performed in the particular order shown or in sequential order, or that all illustrated operations be performed (some operations may be considered optional), to achieve desirable results.

[0044] Accordingly, the previously described example embodiments do not define or constrain this disclosure. Other changes, substitutions, and alterations are also possible without departing from the spirit and scope of this disclosure.

What is claimed is:

1. A composite coaxial fiber comprising:
an inner layer comprising polyacrylonitrile;
an outer layer comprising polyacrylonitrile; and
a middle layer between the inner layer and the outer layer, wherein the middle layer comprises polyacrylonitrile and a multiplicity of glass fibers, wherein the multiplicity of glass fibers are recycled.

2. The composite coaxial fiber of claim **1**, wherein the multiplicity of glass fibers are present in an amount of 0.1 wt % to 200 wt % of the polyacrylonitrile in the middle layer.

3. The composite coaxial fiber of claim **1**, wherein a diameter of the composite coaxial fiber is in a range of about 50 μm to about 250 μm.

4. The composite coaxial fiber of claim **1**, wherein the middle layer has a thickness corresponding to the thickness of a single glass fiber of the multiplicity of glass fibers.

5. The composite coaxial fiber of claim **1**, wherein the multiplicity of glass fibers are aligned along a longitudinal axis of the composite coaxial fiber.

6. The composite coaxial fiber of claim **1**, wherein a draw ratio of the composite coaxial fiber is in a range from about 15 to about 65.

7. A method manufacturing a composite coaxial fiber, the method comprising:
providing a first polymer composition, a second polymer composition, and a third polymer composition to a spinneret to yield a composite coaxial fiber precursor, wherein the first, second, and third polymer compositions comprise polyacrylonitrile, the second polymer composition further comprises recycled glass fibers, and a layered precursor comprises coaxial layers of the first, second, and third polymer compositions, wherein a middle layer of the composite coaxial fiber precursor comprises the second polymer composition;
passing the composite coaxial fiber precursor through an air gap and into a coagulation bath to yield a coagulated composite coaxial fiber precursor;
drawing the coagulated composite coaxial fiber precursor through a heated liquid to align the recycled glass fibers in a middle layer of the coagulated composite coaxial fiber precursor, thereby yielding a drawn coagulated composite coaxial fiber precursor; and
heating the drawn coagulated composite coaxial fiber precursor to yield the composite coaxial fiber, wherein an inner layer, the middle layer, and an outer layer of the composite coaxial fiber comprises polyacrylonitrile, and the middle layer further comprises the aligned recycled glass fibers.

8. The method of claim **7**, wherein the first, second, and third polymer compositions comprise about 5 wt % to about 15 wt % polyacrylonitrile in a solvent.

9. The method of claim **8**, wherein the solvent comprises dimethylformamide.

10. The method of claim **8**, wherein the second polymer composition comprises about 0.1 wt % to about 200 wt % of the recycled glass fibers with respect to the weight of the polyacrylonitrile.

11. The method of claim **7**, wherein a flow rate of passing the composite coaxial fiber precursor through an airgap and into a coagulation bath is in a range of about 1 ml/min to about 3 ml/min.

12. The method of claim **7**, wherein a length of the air gap is about 1 cm to about 3 cm.

13. The method of claim **7**, wherein the coagulation bath comprises methanol.

14. The method of claim **7**, wherein the heated liquid comprises a water bath, an oil bath, or both.

15. The method of claim **14**, wherein an oil in the oil bath comprises a silicone oil.

16. The method of claim **14**, wherein a temperature of the water bath is in a range of about 80° C. to about 90° C. and a temperature of the oil bath is in a range of about 120° C. to about 150° C.

17. The method of claim **7**, wherein a draw ratio of the coagulated composite coaxial fiber precursor is in a range of about 15 to about 65.

18. The method of claim **7**, wherein heating the drawn coagulated composite coaxial fiber precursor comprises heating the drawn coagulated composite coaxial fiber precursor to a temperature in a range of about 250° C. to about 350° C.

19. The method of claim **18**, wherein the heating comprises heating at different rates for 1.5 hours and later cooling to room temperature at a rate of 1° C. per minute.

20. The method of claim **7**, wherein a diameter of the composite coaxial fiber is in a range of about 50 μm to about 250 μm.

21. A method of recycling wind turbine blades, the method comprising:

shredding, crushing, and milling the wind turbine blades to yield a multiplicity of particles comprising glass fiber; and

sieving the particles to yield a multiplicity of pellets comprising glass fiber.

* * * * *